Summary of Meteorological Field Experiments in the Taklimakan Desert, China*

HE Qing, JIN Lili

(*Taklimakan Desert Meteorology Field Experiment Station of CMA, Institute of Desert Meteorology, China Meteorological Administration, Urumqi Xinjiang 830002, China*)

Abstract: In this paper, the latest progress of meteorological research in Taklimakan desert is summarized. On the basis of summarizing the progress of desert meteorology in recent years, the scientific problems of desert weather and climate are discussed, desert land-air interaction, desert atmospheric environment in Taklimakan Desert meteorology field scientific experiment base are explored, and the key scientific problems faced by Taklimakan Desert field scientific experiment results are summarized. Based on multi-scale land-air interaction over rugged terrain, the characteristics and parameterization of sand dust weather, the basic ideas of the key scientific problems of Taklimakan Desert meteorology are discussed, and some preliminary suggestions for further research on Taklimakan Desert meteorology are proposed.

Key words: Taklimakan Desert; Field Atmospheric Scientific Experiment; Land Surface Process; Physics of Blown Sand; Atmospheric Environment

DOI：10.13568/j.cnki.651094.651316.2020.06.02.0001

CLC number：P467 **Document Code**：A **Article ID**：2096-7675(2021)03-0334-21

Citation format：HE Q, JIN L L. Summary of meteorological field experiments in the Taklimakan desert, China[J]. Journal of Xinjiang University(Natural Science Edition in Chinese and English), 2021, 38(3): 334-354.

0 Introduction

The Taklimakan Desert with an area of 33.76 $\times 10^4$ km^2, is the largest desert in China, located in the vast areas of between north latitude 37°~41°and east longitude 77°~90°, in the Tarim Basin in the southern Xinjiang of China, it is 1 070 km long from east to west and 410 km wide from south to north[1]. The sand-dust weather in Taklimakan Desert lasts for a long time, spans the whole spring and summer seasons, and the westerly belt can bring the dust formed by the extremely strong dust storm to thousands of kilometers away, which has a direct impact on the climate and environment changes.

Since the 1980s, based on short-term observations, Chinese scientists have successively carried out research on the Taklimakan Desert, and achieved basic achievements in the field of desert climate. Since its establishment in 2002, Urumqi Institute of Desert Meteorology of China Meteorological Administration has carried out field observations on sandstorm weather with different intensities in the Taklimakan Desert, and obtained the grading test indicators of sandstorm. Since 2005, with the joint support of the China Meteorological Administration and the Ministry of Finance, the Urumqi Institute of Desert Meteorology of the China Meteorological Administration has successively established experimental stations for meteorological observation of desert boundary layer and wind sand observation experimental fields in the Taklimakan Desert, Gurbantunggut Desert and Badain Jaran Desert (in Inner Mongolia Autonomous Region, China), and it has built the Atmospheric Observation Network of the near surface boundary layer in the North-South longitudinal section, which provides the key technical support for the major disastrous weather forecast and early warning in the desert and its surrounding areas. With the establishment of the desert atmosphere comprehensive observation and research platform, the research and development of boundary layer detection technology and integrated method has become suitable for desert area, as well as suitable for the systematic monitoring data and theoretical research of desert boundary layer Many problems such as the inhomogeneity of

* **Received Date**：2020-06-02

Foundation Item：This study was supported by the National Natural Science Foundation of China (41830968; 42030612).

Biography：HE Qing(1965-), Male, Doctor, Researcher, Engage in research on desert meteorology, E-mail: qinghe@idm.cn .

desert undulating surface, the understanding of structure change from near surface layer to boundary layer, and the role of desert land surface process in the climate system have been gradually solved. At the same time, observation experiments on desert land-atmosphere interactions and sand transport processes were used to develop and parameterize a numerical model of desert land surface processes, so as to provide basic data and technical support for the refined observation of catastrophic desert weather and to improve mesoscale numerical predicting models.

Therefore, this paper attempts to summarize the research achievements and key scientific problems of Taklimakan Desert meteorology on the basis of in-depth thinking about the field scientific experiments and related scientific problems of Taklimakan Desert meteorology, and preliminarily proposed the basic ideas to solve the key scientific problems of desert meteorology on non-uniform underlying surface. It will provide a reference for further research on desert meteorology in the future.

1 The Scientific Experimental Base of Taklimakan Desert Meteorological Field

The Scientific Testing Base of Taklimakan Desert Meteorological Field of the China Meteorological Administration is located in the Tazhong Petroleum Operation Area in the hinterland of the Taklimakan desert, with a geographical location of 38 ° 58′N, 83 ° 39′ E, 1 099.3 m above sea level. The experimental base was established in July 1996 and incorporated into the National Basic Meteorological Station of China Meteorological Administration on January 1, 1999. In 2002, the Tazhong Atmospheric Environment Observation Experimental Station of Urumqi Desert Meteorological Institute of China Meteorological Administration was established and incorporated into the National Benchmark Meteorological Station of China Meteorological Administration in 2008. At present, the station has been continuously observed for more than 20 years. The observation results of meteorological field experiment base in Taklimakan Desert of China Meteorological Administration may represent the basic characteristics of atmospheric physics and atmospheric environment in Taklimakan Desert. The experimental base has representative and reference value for the study of land air interaction on the underlying surface of mobile desert, desert boundary layer and turbulence, desert atmospheric composition concentration and its change. It is an ideal experimental site for the study of physical process of atmospheric boundary layer of mobile desert, land surface process of quicksand and dust atmospheric environment. Based on the whole boundary layer detection and a variety of experimental data analysis, the structure characteristics of desert weather system obtained from the test base have good regional representativeness in southern Xinjiang, China. Therefore, the long-term desert positioning observation will effectively promote the basic and applied research in the field of desert meteorology.

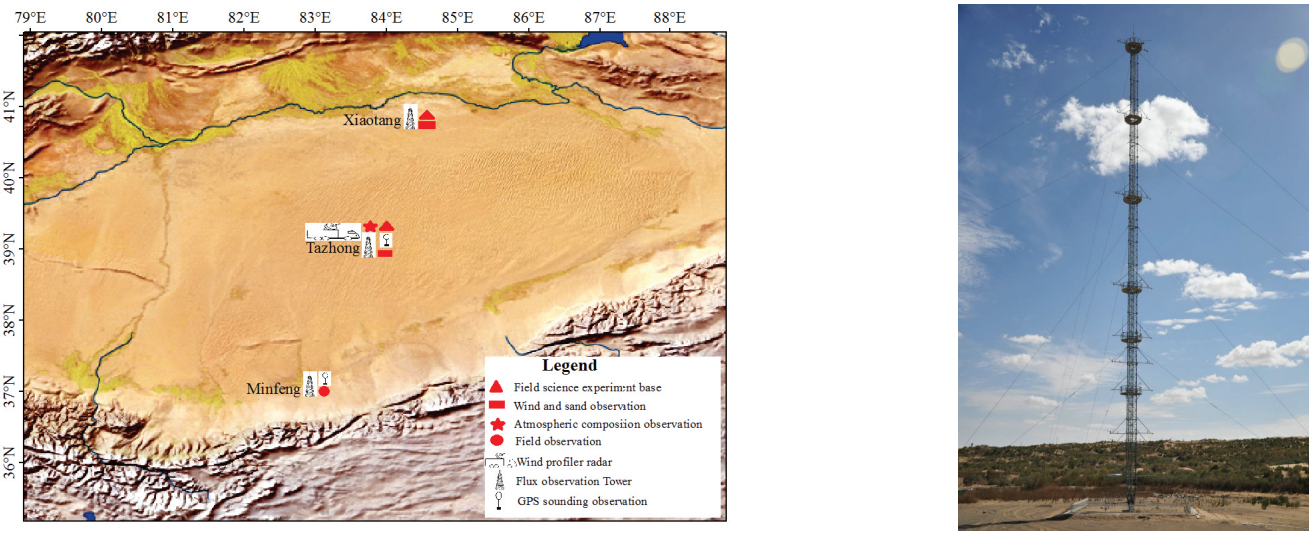

Fig 1 Location of meteorological field test base in the Taklimakan desert

Since 2005, with the support of the China Meteorological Administration and the Ministry of Finance, the 80 m gradient tower flux detection system, radiation detection system and eddy correlation detection system have been established in order to observe the surface structure, water and heat flux exchange and surface radiation energy budget of Taklimakan Desert. At the same time, the tethered airship detection system, wind profile radar detection system and UAV were introduced to detect the meteorological elements and vertical distribution of dust concentration in the boundary layer. In 2016, with the support of the Ministry of Finance, a 100 m gradient iron tower flux detection system (40 ° 49′N, 84 ° 18 ′ E, 932 m above sea level), was established, and it built the boundary layer detection and contrast system in the hinterland of desert and the northern transitional zone.

2 Overview of Meteorological Achievements in Taklimakan Desert

Since the 1970s, a group of scientists led by Charney J G has studied the dynamic mechanisms of arid climate formation such as albedo and heat balance in the Sahara Desert and the Sahel, and they found that high albedo causes the desert heat sinks, which leads to the decrease of precipitation[2,3]. Since the 1980s, Henderson-Sellers[4] and Cunnington[5] have carried out detailed analysis and research on the albedo of different underlying surfaces; Hwang [6] studied the effect of soil moisture on the surface energy balance of bare soil; Thomas T. Warner's [7] study covered all aspects of desert climate, including the causes of large-scale and local-scale drought, desert precipitation characteristics, sandstorm, desert climate change, desertification, desert land surface physics, numerical simulation of desert atmosphere and the impact of desert climate on human beings, and it provided a summary of climate and surface attributes of desert regions in the world.

Since the 1930s, the research methods on sandstorm or sandstorm movement have made great progress. Bagnold's works laid the foundation for the study of aeolian sand physics[8]. Before the 1970s, these experimental methods mentioned above were the mainstream tools for the study on sandstorm or its movement, and were used by Chepil[9], Yakubov[10], Hecun Malone[11], Zingg[12], Owen[13] etc. In the late 1980s, especially since the 1990s, due to the development of science and technology, high-frequency, automated, small-scale monitoring instruments have been used in the research of sand movement, such as high-speed photography monitoring system[14].

Some researches on the interaction between boundary layer and atmosphere in the early stage were carried out in Xinjiang where is the largest desert area of China, but it mainly limited with the area of desert fringe. Since the 1980s, the comprehensive scientific investigation and research on the Taklimakan Desert mainly studied the severe environmental problems in the desert, such as sandstorm, dust tornado, sandstorm, strong drought, high temperature, severe cold, strong light radiation and so on, and preliminarily the weather climate dynamics and thermal mechanism of the Taklimakan Desert were understood.

2.1 Desert climate and sand-dust environment

The climate of Taklimakan Desert in recent 50 years showed an obvious trend of "warming and wetting". The annual average temperature increased abruptly in 1970, the precipitation showed an increasing trend, the number of precipitation days showed a decreasing trend, the precipitation increased abruptly in 1981, while the potential evapotranspiration and surface dryness decreased abruptly in 1981. Temperature, precipitation, potential evapotranspiration and surface dryness have periodic changes on quasi-3-year, 8-year and 16-23-year interannual scales, respectively[15,16].

In the hinterland of Taklimakan Desert, the days of floating dust and blowing sand were on the rise, while the days of sandstorm were on the decline, from January 2004 to December 2009. In spring and summer, the dust weather is frequent, and the monthly average mass concentration of Total Suspended Particles (TSP) mainly concentrated in March to September, with the highest concentration in April and May (the average monthly mass concentration of PM_{10} at the height of 4 m is 846.0 $\mu g \cdot m^{-3}$), and then decreased gradually Most of the sandstorms in Taklimakan Desert are systematic. During the sandstorm, the concentration of dust particles is the highest, and the greater the wind speed is, the higher the particle concentration is. The concentration of PM_{10} at 80 m height is much higher than that of $PM_{2.5}$ and $PM_{1.0}$, while the mass concentration of $PM_{2.5}$ and $PM_{1.0}$ at 80 m height is significantly lower than that at 4 m height, and the daily variation of dust concentration is completely

consistent with the diurnal variation of wind speed[17−21]. When the wind speed reaches at 3.6 m · s^{-1}, the concentration of black carbon aerosol begin to increase with the wind speed, and there are obvious differences in the concentration level of black carbon aerosol under different wind directions[22−24]

The dust aerosols which are transported into the air changes the absorption and energy distribution of solar radiation on the surface. This special weather condition inevitably makes the thermal effect of Taklimakan Desert, which bring its own particularity[25]. The aerosol in the hinterland of Taklimakan desert has the largest scattering effect at the solar radiation of635 nm, followed by 525 nm and the smallest at 450 nm. The daily change of the three-band scattering coefficient is consistent with the PM_{10} mass concentration, showing a single peak variation: higher at night and lower during the day; the annual change of those three-band scattering coefficient is basically the same, which is close to that of PM_{10}; the three-band scattering coefficient is the largest under sandstorm, the second is blowing sand, and the smallest is floating dust; there is a significant positive correlation between those three-band scattering coefficient and mass concentration of PM_{10}. The correlation between PM_{10} mass concentration and 525 nm scattering coefficient is the largest, followed by 450 nm and 635 nm[26−28]. In the two main areas (Pishan-Hetian-Minfeng and Xiaotang-Tazhong), sand-dust events occurs more than 80 days per year. The center of sandstorm is in the north part of the desert (Xiaotang, 46.9 days), but the center of sand-blowing(Pishan, 86.4 days) and the area with frequent floating dust events (Minfeng, 113.5 days) are located in the southwest and the south edge of the desert respectively. The occurrence of sandstorm generally decreased from 1961 to 2010, and the occurrence of blowing sand showed an upward trend from 1961 to 1979, and then decreased as a whole. The main reason is that the temporal changes of sand-dust events are mainly affected by strong winds and daily temperatures, the average correlation coefficients are 0.46 and 0.41 for these variables respectively[29].

2.2 Desert land-air interaction

2.2.1 Atmospheric boundary layer of Desert

In the field of atmospheric boundary layer of desert, scholars at home and abroad have carried out a number of researches and achieved some important research results. A deep convective boundary layer up to 5.5 km was observed in the Sahara Desert, with a clear structure of the residual layer[30]. A convective boundary layer over 4 000 m thick was observed in the Hexi Corridor area of China[31]. The structure of the “cold island effect” was firstly discovered in the oasis of the boundary layer in the arid zone in the 1980s. Hu Yinqiao et al [33] discovered the phenomenon of inverse humidity in the desert atmosphere near an oasis in the “Heihe Experiment” in the 1990s, and the characteristics of the thermal inner boundary layer under the interaction between the oasis and the desert were summarized. In Dunhuang, China, it is found that there was a convective boundary layer with a thickness of more than 4 000 m in the clear sky in summer, and the height of the stable boundary layer at night might also exceed 1 000 m[34−37]. The convective mixing layer in the Badain Jaran Desert of China may reach 3 000 m in summer[38].

In the hinterland of Taklimakan Desert, the development of clear skyturbulence is intense in summer, and the development of convective boundary layer is very profound, with the maximum height up to 4 km[39−41], and the monthly average thickness of the stable boundary layer is 570 m, the residual mixed layer (RML) is 2 700 m and the top cover of residual inversion layer is 350 m respectively[42]. There are strong “cold island effects” and “wet island effects” in artificial green spaces in the desert hinterland [43]. The local microclimate in the center and fringe of the artificial greenbelt in the hinterland of the Taklimakan Desert is mainly manifested in high wind speed and humidity in spring, summer and autumn, while temperature and humidity in winter are mainly affected by inverse temperature and inverse humidity [44].

2.2.2 Land surface processes of desert

In the hinterland of Taklimakan Desert, there is inversion phenomenon in the near surface layer at night in summer, and the change of daytime temperature is opposite; the surface radiation balance is mainly positive, and the surface heat exchange is dominated by turbulent influenza heat. The surface sensible heat and latent heat change with the fluctuation of the solar altitude angle. The maximum value of latent heat appears in the early morning, and the peak value of sensible heat appears at noon[45]. The distribution of sensible heat flux and latent heat flux on the surface of Taklimakan desert exhibits great seasonal

and regional differences. In spring, the sensible heat flux tends to decrease in the north of the desert, and increase in the south. In spring, the latent heat flux tends to decrease in the north and northwest of the desert, and increase in the south and southeast of the desert, while the trend in winter, summer and autumn is not very obvious[46−47]; The surface heat transfer between artificial green land and natural sand surface in desert hinterland is mainly sensible heat transfer, but the sensible heat flux of natural sand surface is higher and the latent heat flux is lower[48].

2.2.2.1 Solar radiation of desert

The Taklimakan desert is rarely affected by human activities, and the influencing factors of solar radiation are mainly related to clouds and dust aerosols[49]. The average annual amount of total radiation, scattered radiation and horizontal direct radiation in the hinterland of Taklimakan Desert are 6 619 MJ · m^{-2}, 3 507.8 MJ · m^{-2} and 2 203.5 MJ · m^{-2}, respectively. The daily peak values of total radiation in typical sunny days are 2.4 times of scattered radiation and 1.5 times of direct radiation, respectively. The increased value of scattered radiation in sandstorm days is basically consistent with the total radiation[50]. The scattering radiation in the desert hinterland increases in autumn and winter, raises exponentially with the rise of solar altitude angle, and decreases rapidly with the increase of atmospheric quality [51]. The average annual total ultraviolet radiation in the desert hinterland is 320.7 MJ · m^{-2}, with the maximum value of 62.5 w · m^{-2} (June) and the minimum value of 29.3 w · m^{-2} (December); the annual total UV-B radiation is 8.59 MJ · m^{-2}, and the annual peak is 2.51 w ·m^{-2} in June. The frequent occurrence of sand-dust weather in spring and summer leads the conspicuous fluctuation of diurnal variation of ultraviolet radiation. In floating dusty days, sandy sky days and sand-dusty days, the relative attenuation of ultraviolet radiation is 26%, 38% and 45% respectively. The attenuation of ultraviolet radiation caused by sand-dust weather is 2~4 times than that of caused by cloud cover weather[52−53].

2.2.2.2 Thermal effect of desert and soil

The average soil heat capacity, thermal conductivity and thermal diffusivity in the hinterland of Taklimakan Desert are 1.559（± 0.140）× 10^6 J·$m^{-3}K^{-1}$, 0.234（± 021) w · M^{-1}· k^{-1} and 1.504（± 0.110）× 10^7 $m^{-2}s^{-1}$ respectively; Soil heat capacity and heat conductivity present obvious seasonal changes, with stable low values in winter and unstable high values in summer[54]. The surface emissivity of Taklimakan desert is the highest near the oasis, reaching 0.93, the value of oasis desert transition zone is 0.91 ~ 0.92, the value of other desert areas is 0.90 ~ 0.91, and the value of desert hinterland area is less than 0.90[55]. The annual average value of surface albedo in the hinterland and northern edge of Taklimakan desert is 0.27[56], and the daily average value of albedo has obvious seasonal variation, which is higher in winter and lower in summer. The daily variation of surface albedo with snow cover is varied 0.18~0.97, daily average value is 0.60, more inclined to reverse "J" type, showing a pattern that morning is higher than evening, and the average difference between morning and evening is 0.13. There was a negative correlation between snow albedo and surface temperature, the correlation coefficient was - 0.71, and a negative correlation between snow albedo and soil moisture at 5 cm depth, the correlation coefficient was -0.74[57]. The surface albedo is varied in different weather in the northern edge of Taklimakan Desert, and it decreases in rainy days and increases in snowy days. When the clearness index is <0.3, the surface albedo fluctuates greatly. Soil moisture impacts on the daily variation of surface albedo in the northern edge of the desert, and the surface albedo is sensitive to the shallow soil moisture in the range of 0.097-0.13[56]. Surface albedo on the northern edge of desert (α) and specific emissivity(ε) are 0.27 and 0. 91 respectively, which are consistent with the values of Taklimakan Desert hinterland and North American Basin Desert, and α and ε values can be obtained from remote sensing products[58].

The annual average value of soil heat flux at 1 cm in the hinterland of Taklimakan desert is 1.9 w · m^{-2}, the annual maximum value is 334.1 w · m^{-2}, and the annual minimum value is -184.2 w · m^{-2}; The basic featureis summer > spring > autumn > winter, each soil layer of soil heat flux shows obvious diurnal variation characteristics, and there are certain differences in diurnal variation characteristics under different weather conditions, and it is most significantly affected by the weather at soil depth of 1 cm[59]. On the daily variation scale, the soil heat flux in the hinterland and the northern edge of the desert has obvious diurnal variation characteristics. The daily average variation of the soil heat flux in the hinterland of the desert is less than that in the northern edge in January , in April they are relatively close, and in July and October the variation

range of the soil heat flux in the hinterland of the desert is significantly higher than that in the northern edge [60].

2.2.2.3 Concentration of carbon dioxide and ozone in desert

In the hinterland of the Taklimakan Desert, the land surface absorbs CO_2 in the daytime and emits CO_2 at night, and the surface absorption intensity is significantly greater than the surface emission, and the CO_2 flux is greatly affected by the atmospheric stability[61]. The soil respiration rate in the hinterland of desert is generally slow, but it shows obvious diurnal fluctuation and seasonal variation characteristics[62]. However, the soil respiration rate of saline alkali land and quicksand land in the northern edge of desert is relatively slow [63]. There is interaction between the soil respiration and weak meteorological conditions, and they jointly regulate and control the variation of CO_2 concentration in the near surface layer[64]. The diurnal variation of soil respiration in winter showed a significant unimodal curve. There is extremely significant or significant positive linear relationship between soil respiration, air temperature in each layer and surface temperature at 0 cm, and it had obvious linear relationship with soil moisture at 5 cm, and surface temperature at 0 cm had the greatest contribution to it[65].

The concentration of surface ozone in the hinterland of Taklimakan Desert ranges from 33.8 $g \cdot m^{-3}$ to 65.3 $g \cdot m^{-3}$, with an average concentration of 49.0 $g{\cdot}m^{-3} \pm 0.45$ $g{\cdot}m^{-3}$; The change of ozone concentration shows weekend effect, which is smooth at night and dramatic during the day, reaching the lowest value around 09:00 and the highest value around 18:00. During the sandstorm, the ozone concentration decreases significantly[18]

2.2.2.4 Key parameters of desert land surface process

The range of dynamic roughness in the hinterland of the Taklimakan Desert is 2.7×10^{-5} m~8.0×10^{-5} m, and it reaches 21.04×10^{-5} m~91.32×10^{-5} m in winter[54]. The peak value of dynamic roughness (z_{0m}) is 5.858×10^{-3}m, which is similar to Mojave Desert, Peruvian desert, Sonoran desert, Heihe desert and Badain Jaran Desert. In the north of the Taklimakan Desert, the peak value of thermodynamic roughness (z_{0h}) is 1.965×10^{-4} m, which is different from the hinterland of Taklimakan Desert. The annual average additional damping of heat transfer (kB^{-1}) is 2.5, which is different from HEIFE Gobi and desert, but similar to Qinghai Tibet Plateau and HAPEX desert steppe. The diurnal variation of z_{0m} and z_{0h} is not obvious, but the seasonal variation is obvious. The diurnal variation and seasonal variation of kB^{-1} are not obvious. z_{0m} is obviously affected by local wind direction. There are many undulating dunes in the prevailing and counter prevailing wind directions, which are consistent with the peak direction of z_{0m}. The daily average values (24 hours) of turbulent dynamic transport coefficient (C_d) and turbulent thermal transport coefficient (C_h) are 6.34×10^3 and 5.96×10^3, respectively , which is higher than the hinterland of Taklimakan Desert and gobi region, and similar to HEIFE desert. Under the prevailing wind direction (NNE – ESE), according to the similarity theory, the average C_d and C_h have the same magnitude. Under different wind directions, the relationship between C_d and C_h, wind speed (U)and stability parameter (Z / L)are different. When the wind speed is lower than 3 $m \cdot s^{-1}$ and its minimum value is 1 $m \cdot s^{-1}$~2 $m \cdot s^{-1}$, C_d and C_h decrease rapidly. It should be pointed out that using sensible heat flux estimation is more important than using other estimation methods when obtaining the value of (ε)[58].

2.2.2.5 Turbulent flow of desert

Under weak instability or near neutral condition the scale of characteristic length of turbulent vortex in desert hinterland is the largest, and it decreases with the increase of instability, with the increase of stability it firstly decreases rapidly and then decreases slowly. The wind speed of near ground layer decreases firstly and then increases during the sandstorm transit. The downward transport of momentum is obvious at 10 m height, and the heat transfer shows slower rising tendency; Before the sandstorm passing through, the near ground is a weak and stable inversion layer, and the air is in a state of warm-dry condition. The vertical air flow at 10 m height shows a systematic downward movement. With the sandstorm outbreak, the turbulence exchange is significantly enhanced, and the air flow shows an upward movement trend, however the intensity is not large, and it still dominated by the horizontal turbulence energy[67].

In most cases, the distribution of turbulence velocity spectrum in the northern margin of desert meets the exponential rate of -2/3, and the degree of compliance of inertial sub region in high frequency section in vertical direction is higher, followed by horizontal direction; The concentration of CO_2 and H_2O was lower; In general the temperature spectrum has a good correlation with dimensionless frequency. In most cases the fitting value of the co spectral slope of vertical wind speed

and radial wind speed is closer to - 1, and more in line with - 4/5 oblique line in near neutral stratification condition. The peak value of the co spectrum is larger and about one magnitude under the stable layer junction than that of the unstable layer junction; The high frequency band co spectrum decreases in the near linear mode under the condition of unstable stratification. The peak wavelength of u spectrum decreases with the increase of stability, while the peak wavelength of V spectrum and t spectrum do not increase or decrease regularly with the increase of stability; The peak wavelengths of U, V, W and T are about 67 m~827 m, 69 m~2 417 m, 4 m~54 m and 12 m~661 m, respectively[68].

2.3 Study on Aeolian Sand Physics

2.3.1 Characteristics of surface environmental

The average grain size of surface soil in Taklimakan desert is 15.6 μm~250 μm. It consists of fine sand (125 μm~250 μm), very fine sand (62.5 μm~125 μm), coarse silt (31 μm~62.5 μm) or its mixture[69]. The sand transported by aeolian sand flow in the hinterland of the desert and the adjacent strata(below 2 m height) of the northern margin is mainly fine sand (125 μm~250 μm),very fine sand (62.5 μm~125 μm),most of them are fine sand, accounting for 43.8 %~75.5% of the sediment transport. The content of coarse sand(> 250 μm) in each height layer is very little[70]. The average grain size of sand transported by aeolian sand flow is 62.5 μm~125 μm, the average grain size of 5 cm near the ground is the largest, and that of 2 m is the smallest, which indicates that the smaller grain size can jump higher under the same conditions[71].

In the hinterland of Taklimakan Desert, sand with grain size larger than 0.3 mm has better transparency, and there are also a small number of sand particles with poor transparency, such as red and black sand particles. The surface abrasion of those sand particles is more obvious, the edges and corners are less, and the roundness is better. The distribution of roundness value is relatively concentrated, mostly between 0.7 and 1.0, and the proportion of sand particles with roundness value between 0.8 and 0.9 is the largest, especially at the height of 5 cm, 10 cm and 200 cm; there are various shapes of sand particles with the size of 0.125 mm~0.3 mm. The roundness values of sand particles are concentrated in the range of 0.7 ~ 1.0, and 41.49% of them are less than 0.7; Among the sand particles with grain size between 0.074 mm and 0.125 mm, the number of strip sand particles increases, the shape of sand particles becomes more complex, the surface abrasion becomes lighter, and the edges and corners become sharper [72].

2.3.2 Study on wind blown sand flux

In the hinterland of Taklimakan Desert, the structure of 0 cm~100 cm aeolian sand flow completely conforms to the exponential distribution, but there is no such characteristic in the northern margin. The grain size of aeolian sand flow is mainly fine sand, very fine sand and silty sand, of which the very fine sand accounts for 43.8%~75.5% of the total amount. The amount of sand transport has a downward trend with the increase of altitude. The sand movement in the desert hinterland is mainly concentrated in the range of 20 cm~30 cm near the surface. The amount of sand transported by 0 cm can be used as the amount of creeping sand, and the amount of creeping sand accounts for the total amount of sand transport the proportion is about 11.6%. There is a big difference between the direction distribution of creeping sand transport and the wind direction distribution. The wind speed profile of the ground layer in the wind-sand flow is affected by the interaction of wind-sand, and no longer conforms to the logarithmic distribution. It is more in line with the power function distribution($u = az^b$), and the fitting coefficients are all greater than 0.93[70,71].

In the desert hinterland, the wind direction of sand onset wind and sand transport potential are mainly distributed in ENE, NE and E directions[73]. In the process of sand-dust weather (sandstorm and sand blowing), with the increase of wind speed, the sand transport at each height also increases. In the two weather processes, the average grain size of sand firstly decreases and then increases in the vertical height. Using the data of H-sensit wind erosion sensor, anemometer and micro gradient sediment collection instrument, it is found that in the range of 85 mm height, with the increase of wind speed, the ratio of jump amount/creep amount decreases in a negative power function. When the wind speed is about 8.5 $m \cdot s^{-1}$, the ratio of jump amount/ creep amount is about 8~10; When the wind speed reaches 6.9 $m \cdot s^{-1}$, the maximum jump is 1 952.01 g; When the wind speed reaches 7.6 $m \cdot s^{-1}$, the maximum creep is 211.79 g. The ratio of total jump to total creep decreases exponentially with the increase of wind speed. The ratio of total jump to total creep at different wind speeds in a typical

weather process is about 8~24. With the increase of wind speed, the sediment transport is more and more concentrated in the range of 0 mm~35 mm. There is a good linear relationship between the total amount of sand collection and the number of saltation particles recorded by the Sensit wind erosion sensor the average R^2 value is 0.605 3, the average sand collection efficiency of the automatic sand collector at the height of 5 cm is 94.3%. During the observation period, there are significant differences in the amount of sand-dust transported by different sand dust weather processes. The maximum horizontal flux of sand-dust in a cross section of 2 cm (wide) × 5 cm (high) is about 190.335 kg, and the minimum is 1.2 kg. In dusty weather, the maximum sand transport rate appears at a height of 5 mm~15 mm, and the minimum appears at a height of 35 mm~85 mm. In the sand blowing weather, when the wind speed is greater than 9.2 $m \cdot s^{-1}$, the maximum sediment transport rate is 0 mm~5 mm. In sandstorm weather, the inflection point wind speed is 7.5 $m \cdot s^{-1}$.When it is less than 7.5 $m \cdot s^{-1}$, the increase of sand transport rate is not significant, when it is greater than 7.5 $m \cdot s^{-1}$, the increase of sand transport rate is significant[74−78]. Using BSNE sand collector, it was observed that the horizontal flux of sand dust on the top of sand dune and flat sand decreased significantly with height. Under these two underlying surface conditions, the change of horizontal flux of sand dust with height was in good accordance with the power function relationship[79].

The vertical sand flux increases with the rise of wind speed, and the maximum flux is concentrated in the afternoon. When it is 2 m and the wind speed is 2 $m \cdot s^{-1}$, the vertical sand dust flux in the hinterland and the northern edge of the desert is close to 3 $kg \cdot m^{-2}$. When it is 2 m and the wind speed is 6 $m \cdot s^{-1}$, the vertical sand dust flux in the hinterland and the northern edge of the desert is 10 $kg \cdot m^{-2}$. When the wind speed is 2 $m \cdot s^{-1}$, the horizontal dust flux in the hinterland and north edge is about 20 $kg \cdot m^{-2}$, and the value in the hinterland is slightly larger. When the wind speed is 4 $m \cdot s^{-1}$, the horizontal dust flux in the hinterland and north edge is about 40 $kg \cdot m^{-2}$, and the value in the hinterland is larger. When the wind speed is 6 $m \cdot s^{-1}$, the horizontal dust flux in the hinterland is about 70 $kg \cdot m^{-2}$, and the horizontal dust flux in the northern margin is about 65 $kg \cdot m^{-2}$ [80].

The average particle size of Sandstorm in the hinterland of desert is 70 μm~85 μm. Because of the existence of sand dunes and valleys, the horizontal dust flux increases with the increase of height in the lower altitude, but remains unchanged when it exceeds above 32 m. The vertical distribution of boundary layer is controlled by wind speed, and the average flux varies from 8 $kg \cdot m^{-2}$ to 14 $kg \cdot m^{-2}$. The size of dust particles PM_{100} and below accounts for 60 %~80% of the collected samples, in which $PM_{0-2.5}$ is 0.9 %~2.5%, PM_{0-10} is 3.5%~7.0%, PM_{0-20} is 5.0 %~14.0%, and PM_{0-50} is 20 %~40%. The average vertical flux potential of dust is about 0.29 $kg \cdot m^2$, and particles smaller than PM_{20} are transported from 80 m to the upper boundary layer and free atmosphere of the planet[81].

2.3.3 Transport mechanism of near surface sediment

In the hinterland of Taklimakan Desert, the climate factor index of annual average wind erosion (the main index to evaluate the potential wind erosion capacity of a certain area) is 28.3, 13.9 in summer, 0.7 in winter, and the average surface roughness is 6.32×10^{-5} m, the surface roughness is small, which aggravates the degree of wind erosion of soil in this area[82]. The critical friction velocity in the hinterland of the Taklimakan desert is 0.24 $m \cdot s^{-1}$. Yang Xinghua et al[83] found that the calculated results of the Lettau formula were the closest to the measured values. The critical friction velocity was 0.26 $m \cdot s^{-1}$ in spring and summer, and the critical wind velocity was about 4.1 $m \cdot s^{-1}$ at 2 m height; The change of dust flux was consistent with the change of wind speed and friction velocity. Zhou Chenglong et al[73] comprehensively considered the surface soil particle size, soil moisture, air density and other factors, and obtained the critical friction velocity (0.24 $m \cdot s^{-1}$~0.36 $m \cdot s^{-1}$) and critical sand blowing velocity (3.9 $m \cdot s^{-1}$~5.9 $m \cdot s^{-1}$, with an average of 5.1 $m \cdot s^{-1}$) at 2 m height in the hinterland of desert; The sand threshold in the desert hinterland was the highest in summer, the second highest in winter and the lowest in spring.

There are some differences in the critical wind speed obtained by different time steps. With the decrease of time step, the critical wind speed is more and more refined. There are different parameterization schemes indifferent values of critical wind speed. Based on Marticorena and Shao schemes,the mean values of critical wind speed are 4.88 $m \cdot s^{-1}$ and 6.24 $m \cdot s^{-1}$, respectively[84−85]. The minimum wind speed and critical starting friction velocity obtained by H11LIN wind erosion sensor

are 6.0 m · s^{-1} and 0.25 m · s^{-1} respectively [86].

The saltation activity of Taklimakan Desert often occurs in the daytime of each season, and the most active time of saltation is about 11:30 local time and lasts about 16:30. From September 1, 2008 to August 31, 2010, the time of jumping activity accounted for more than 3% of the total time of the whole year, and inclined to reach the peak in the windy months of spring and summer. However, it tends to be the smallest in the months when the wind speed is weak in winter. In the extremely arid Tazhong area, precipitation has no significant effect on reducing sand saltation[87−88].

Gauss time fraction method developed by Stout (interval is 1 day), the obtained friction velocity threshold is 3.03 m · s^{-1}~5.62 m · s^{-1} (field test observation method), the value obtained by Kurosak method is 3.71 m · s^{-1}~5.74 m · s^{-1} (statistical calculation method), and the value given by Marticorena and Shao model is 4.87 m · s^{-1}~4.90 m · s^{-1} and 5.82 m · s^{-1}~6.78 m · s^{-1} (model parameterization method)[85]. The total horizontal dust fluxes estimated by Stout, Kurosak, Marticorena and Shao methods are 1 311.9 kg · m^{-1}, 1 166.4 kg · m^{-1}, 1 279.9 kg · m^{-1} and 661.6 kg · m^{-1}, respectively, while the observed values are 732.9 kg · m^{-1}. The correlation coefficients between estimated values and observed values based on Stout, Kurosak, Marticorena and Shao methods are 0.75, 0.79, 0.77 and 0.83, respectively. According to the friction velocity threshold, the duration of sand jumping values estimated by Stout, Kurosak, Marticorena and Shao methods are 8 211 min, 6 575 min, 7 567 min and 3 463 min respectively, while the correct time is 6 208 min, 5 646 min, 5 986 min and 3 346 min respectively.

The threshold of wind velocity(TWV) mainly occurrs in the daytime (08:00~20:00), and in spring (6.4%), summer (5.6%), autumn (1.7%) and winter (0.8%). The DUP increased to 50% on June 17 and 90% on September 1. The DUP was observed from April 1 to July 31 for two consecutive years from September 1, 2008 to August 31, 2010. The result showed that 75.4% DUP was produced. And The results also show that different time resolution of wind speed will affect the calculation of DUP. When the wind speeds are measured for 1 minute, 5 min,10 min and 15 min the DUP are 9.93 ×10^6 $m^3 \cdot s^{-3}$, 8.96× 10^6 $m^3 \cdot s^{-3}$, 8.51 × 10^6 $m^3 \cdot s^{-3}$, 8.32× 10^6 $m^3 \cdot s^{-3}$, × 10^6 $m^3 s^{-3}$, respectivly ; The seasonal variation of DUP was as follows: winter > summer > autumn > spring. By analyzing the diurnal DUP and wind speed in different observation periods, it is found that the main deviation occurs in the morning and evening. If the average wind speed is measured at intervals of 10 minutes or longer, there will be some errors in assessing the damage caused by wind dust activities [89].

3 Conclusion

In the hinterland of the Taklimakan Desert, China Meteorological Administration has established the Tazhong atmospheric environment observation and experimenting station of Urumqi Institute of Desert Meteorology of China Meteorological Administration. It has conducted long-term research on the land-air interaction, the dynamic mechanism of weather and climate formation, the atmospheric environment and the mechanism of surface dust emission and its transportation in the Taklimakan Desert and its surrounding areas, for more than ten years. Systematic achievements have been made in desert climate and environment, desert land-air interaction, aeolian sand physics, etc. However, there are still some problems, such as the imperfection of the system, the lack of revealing and understanding of the problems, the lack of in-depth analysis of all kinds of influencing factors measured in the field, and the insufficient utilization.

In order to meet the increasing needs of national regional development strategy, disaster prevention and mitigation, meteorological services and scientific research, the desert meteorological research requires strengthening the observation and experimenting of land-air interaction and surface sand transportation process, enhancing the application ability of comprehensive observation data, and improving the research of desert climate change characteristics, sand transport law and desert micro meteorological characteristics. At the same time, it is necessary to obtain the key land surface process parameters which is essential to improve the regional numerical prediction model and improve the prediction ability of the model combined with remote sensing technology; It is also necessary to use modern air-space-ground observation methods, combined with big data processing techniques, to conduct in-depth research on the scientific issues such as: the radiative forcing of sand-dust aerosols in desert areas the influencing mechanism of positive and negative feedback effects of the complex coupling system between the desert and the atmosphere.

塔克拉玛干沙漠气象野外科学试验成果概述*

何 清，金莉莉
(中国气象局 乌鲁木齐沙漠气象研究所，塔克拉玛干沙漠气象野外科学试验基地，新疆 乌鲁木齐 830002)

摘　要： 本文综述了塔克拉玛干沙漠气象研究的最新进展. 在总结近年来沙漠气象领域进展的基础上，就塔克拉玛干沙漠气象野外科学试验基地开展的沙漠天气和气候、沙漠陆气相互作用和沙漠大气环境的科学问题进行了探讨，分析和归纳了塔克拉玛干沙漠野外科学试验成果面临的关键科学问题. 以起伏地形多尺度陆气相互作用特征，沙尘天气起沙特征及其参数化等为重点讨论了塔克拉玛干沙漠气象关键问题的基本思路，并对进一步开展塔克拉玛干沙漠气象研究提出了初步的科学建议.

关键词： 塔克拉玛干沙漠；野外大气科学试验；陆面过程；风沙物理；大气环境
DOI： 10.13568/j.cnki.651094.651316. 2020.06.02.0001
中图分类号： P467　**文献标识码：** A　**文章编号：** 2096-7675(2021)03-0334-21
引文格式： 何清, 金莉莉. 塔克拉玛干沙漠气象野外科学试验成果概述[J]. 新疆大学学报（自然科学版）（中英文）, 2021, 38(3): 334-354.

0　引 言

塔克拉玛干沙漠面积33.76×10^4 km^2，是我国最大的沙漠，地理位置处于东经77°～90°、北纬37°～41°之间，位于中国新疆南部塔里木盆地，东西长约1 070 km，南北宽410 km[1]. 塔克拉玛干沙漠沙尘天气发生期持续时间长，跨越了整个春夏季节，而且西风带可以将特强沙尘暴天气形成的沙尘带至数千公里以外，对我国东部区域乃至全球气候和环境的变化都有着直接的影响.

20世纪80年代以来，中国科学家基于短期观测先后开展了有关塔克拉玛干沙漠的考察研究，取得了沙漠气候领域的基础性成果. 中国气象局乌鲁木齐沙漠气象研究所自2002年组建以来，在塔克拉玛干沙漠开展了不同强度沙尘暴天气野外强化观测，获取了沙尘暴的分级试验指标. 自2005年起，在中国气象局和财政部的共同资助下，乌鲁木齐沙漠气象研究所先后在塔克拉玛干沙漠、古尔班通古特沙漠和内蒙古巴丹吉林沙漠建立了以梯度通量塔为核心的沙漠边界层气象观测试验站和风沙观测试验场，建成了南北纵向剖面的近地边界层大气观测网络，为开展沙漠及其周边地区重大灾害性天气预报预警提供了基础资料和关键技术支撑. 随着沙漠大气综合观测研究平台的建立，适用于沙漠地区的边界层探测技术和集成方法的研发，沙漠边界层系统性的监测资料和理论研究，许多诸如沙漠起伏地表非均匀性、近地层到边界层结构变化认识、沙漠陆面过程在气候系统中的作用等问题逐步深入推进，同时，开展沙漠地气相互作用和起沙输送过程观测试验，发展和研究较为准确的描述沙漠陆面过程数值模式和参数化方案，从而为沙漠灾害性天气的精细化观测和中尺度数值预报模式改进提供基础资料和技术支撑.

鉴于此，本文试图对塔克拉玛干沙漠气象野外科学试验及有关科学问题深入思考的基础上，归纳塔克拉玛干沙漠气象取得的研究成果及面临的关键科学问题，初步提出破解非均匀下垫面沙漠气象关键科学问题的基本思路，为今后继续深入开展沙漠气象研究提供参考.

1　塔克拉玛干沙漠气象野外科学试验基地

中国气象局塔克拉玛干沙漠气象野外科学试验基地位于沙漠腹地塔中石油作业区，地理位置为38°58′N，83°39′E，海拔1 099.3 m. 试验基地始建于1996年7月，1999年1月1日正式纳入中国气象局国家基本气象站，2002年建立中国气象局乌鲁木齐沙漠气象研究所塔中大气环境观测试验站，2008年纳入中国气象局国家基准气象站，目前该站是世界上唯一深入流动沙漠腹地200 km以上的大气科学综合观测试验站，该站已连续观测20多年. 中国气象局塔克拉玛干沙漠气象野外科学试验基地观测结果可代表塔克拉玛干沙漠区域的大气物理和大气环

* **收稿日期：** 2020-06-02
基金项目： 国家自然科学基金重点项目(41830968；42030612).
作者简介： 何清（1965-），男，博士，研究员，主要从事沙漠气象研究，E-mail: qinghe@idm.cn.

境基本特征. 基于该试验基地观测资料的对流动性沙漠下垫面陆气相互作用、沙漠边界层与湍流、沙漠大气成分浓度及其变化研究具有代表性和参考价值，是研究流动沙漠大气边界层物理过程、流沙陆面过程、沙尘大气环境十分理想的天然试验场. 该试验基地的全边界层探测及多种试验数据分析得到的沙漠天气系统结构特征在南疆具有区域代表性. 长期的沙漠定位观测将有力地推动我国沙漠气象学领域基础和应用研究工作扎实开展.

2005年以来，在中国气象局和财政部的资助下，以塔克拉玛干沙漠腹地塔中作为试验基地，先后建立了80 m梯度铁塔通量探测系统、辐射探测系统、涡动相关探测系统以用于观测塔克拉玛干沙漠近地层结构、水热通量交换以及地表辐射能量收支. 同时，引入系留气艇探测系统、风廓线雷达探测系统和无人机探测边界层气象要素和沙尘浓度垂直分布. 2016年在财政部的资助下，在塔中以北约220 km处肖塘流沙下垫面建立100 m梯度铁塔通量探测系统（40°49′N、84°18′E，海拔932 m），形成了沙漠腹地和北部过渡带边界层探测对比系统.

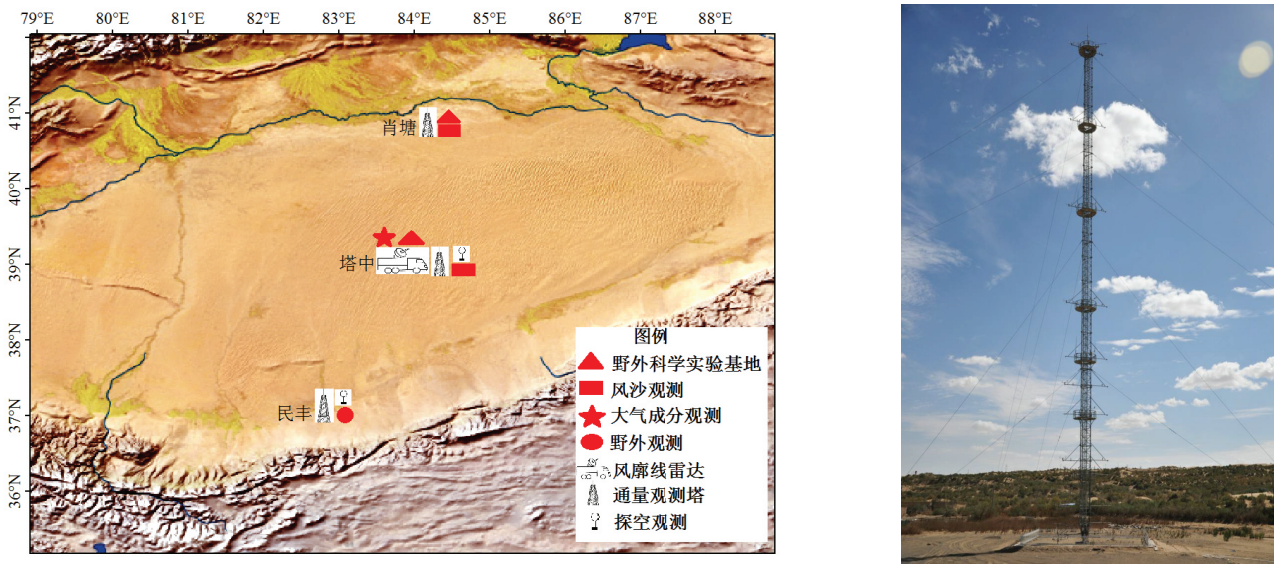

图 1 塔克拉玛干沙漠气象野外科学试验基地位置

2 塔克拉玛干沙漠气象研究成果概述

20世纪70年代以来以Charney为代表的一批科学家对撒哈拉沙漠和萨赫勒地区干旱气候形成动力学机制的反照率、热量平衡等因素做了大量研究，发现高反照率使沙漠形成热汇和空气下沉，从而导致降水减少；反之，则降水增加[2,3]. 20世纪80年代以来，Henderson Sellers[4]、Cunnington[5]等对不同下垫面反照率均进行了细致的分析研究；Hwang[6]进行了土壤湿度对裸露土表面能量平衡影响研究；Warner[7]的研究囊括了沙漠气候的所有方面，内容涉及大尺度和局部尺度干旱的成因、沙漠降水特征、沙尘暴、沙漠气候变化、沙漠化、沙漠陆面物理学、沙漠大气数值模拟及沙漠气候对人类的影响，提供了世界荒漠地区气候和表面属性的概要.

20世纪30年代以来，沙尘暴或风沙运动研究手段有了重要的进展. Bagnold的著作为风沙物理学研究奠定了基础[8]. 这些试验方法在20世纪70年代以前是研究沙尘暴或发生运动的主要手段，被Chepil[9]，雅库波夫[10]，河村龙马[11]，Zingg[12]，Owen[13]等学者沿用. 20世纪80年代后期，特别是20世纪90年代以来，由于科技水平的发展，高频率、自动化、微小尺度的监测仪不断被用于风沙运动的研究中，如高速摄影监测系统等[14].

新疆作为全国荒漠面积最大的省区，有一些学者早期开展了一些边界层与地气相互作用的考察研究，其主要在荒漠边缘区进行. 20世纪80年代以后对塔克拉玛干沙漠进行的综合科学考察研究，主要研究了沙漠中诸如沙尘暴、尘卷风、风沙、强烈干旱、高温、严寒、强光辐射等严酷环境问题，初步认识了塔克拉玛干沙漠天气气候动力和热力机制.

2.1 沙漠气候与沙尘环境

塔克拉玛干沙漠近50年气候总体呈较明显的“暖湿化”趋势，年平均气温在1970年突变性地升高，降水量表现出增加趋势，降水日数呈减小趋势，降水量在1981年突变性地增多，而潜在蒸散量和地表干燥度在1981年

突变性地减小. 气温、降水、潜在蒸散量和地表干燥度分别存在准3 a、8 a的年际尺度和16 a～23 a的年代际尺度的周期性变化[15,16].

2004年1月至2009年12月，塔克拉玛干沙漠腹地浮尘、扬沙日数呈上升趋势，沙尘暴日数呈下降趋势. 春、夏季沙尘天气频繁，总悬浮颗粒物（TSP）月平均质量浓度高值主要集中在3—9月，其中4月和5月浓度最高（4 m高度PM_{10}月平均质量浓度为846.0 $\mu g \cdot m^{-3}$），随后逐渐减低. 塔克拉玛干沙漠的沙尘暴多为系统性沙尘暴，沙尘暴期间沙尘颗粒物浓度最高，且风速越大颗粒物浓度越高，80 m高度PM_{10}浓度远高于$PM_{2.5}$和$PM_{1.0}$浓度，而80 m高度$PM_{2.5}$和$PM_{1.0}$质量浓度明显低于4 m高度的，且沙尘浓度日变化规律与风速的昼夜变化完全一致[17−21]. 风速达到3.6 $m \cdot s^{-1}$之后黑碳气溶胶浓度随风速不断增大，不同风向时黑碳气溶胶浓度水平有较明显的差异[22−24].

沙尘气溶胶输送至空中，改变了太阳辐射在地表的吸收和能量分配，这种特殊的天气背景必然使得塔克拉玛干沙漠的热力作用有其自身的特殊性[25]. 塔克拉玛干沙漠腹地气溶胶对635 nm太阳辐射的散射作用最大，其次是525 nm，最小为450 nm. 以上三波段散射系数日变化与PM_{10}质量浓度一致，呈单峰变化：夜间高、白天低；三波段散射系数年变化基本一致，都与PM_{10}变化接近；三波段散射系数均是沙尘暴下最大，扬沙次之，浮尘最小；三波段散射系数与PM_{10}质量浓度都呈显著正相关，PM_{10}质量浓度与525 nm散射系数相关程度最大，450 nm次之，635 nm最小[26−28].

在沙尘事件集中爆发的两个主要区域（皮山—和田—民丰和肖塘—塔中），平均每年沙尘事件发生天数超过80天. 该地区为沙尘暴、扬沙天气最高的区域，但沙尘天气发生的区域不同，沙尘暴天气的中心在沙漠的北部（肖塘，46.9天），然而扬沙天气的中心位置（皮山，86.4天）及浮尘事件活跃频繁地区（民丰，113.5天）分别位于沙漠的西南部和南部边缘. 1961年至2010年沙尘暴的发生普遍减少，其中1961年至1979年发生扬沙呈上升趋势，随后总体呈减小趋势. 主要是沙尘事件的时间变化受大风和日气温的影响，其平均相关系数分别为0.46和-0.41[29].

2.2　沙漠陆气相互作用

2.2.1　沙漠大气边界层

在沙漠大气边界层领域，国内外学者先后开展了大量的研究，取得了一些重要的研究成果. 撒哈拉沙漠观测到高达5.5 km的深厚对流边界层，并且残余层结构清晰[30]，中国河西走廊地区观测到超过4 000 m厚的对流边界层[31]，且苏从先等[32]于20世纪80年代在干旱区边界层的绿洲首次发现了“冷岛效应”结构. 胡隐樵等[33]在20世纪90年代的“黑河试验”中发现了邻近绿洲的荒漠大气逆湿现象，并总结出绿洲与荒漠相互作用下的热力内边界层特征. 中国敦煌发现该地区夏季晴空会出现超过4 000 m厚的对流边界层，并且夜间稳定边界层高度也可超过1 000 m[34−37]；中国巴丹吉林沙漠在夏季晴天对流混合层可以达到3 000 m高度[38]，而在塔克拉玛干沙漠腹地夏季晴空湍流发展剧烈，对流边界层发展极为深厚，最大高度可达到4 km[39−41]，夜间稳定边界层月平均厚度为570 m、残余混合层的平均厚度为2 700 m，残余逆温层顶盖的平均厚度为350 m[42]. 沙漠腹地人工绿地存在较强的“冷岛效应”和“湿岛效应”[43]. 塔克拉玛干沙漠腹地人工绿地中心和边缘地带局地小气候主要表现在较高的风速和春、夏、秋季湿度上，而气温和冬季湿度分别主要受逆温和逆湿的影响[44].

2.2.2　沙漠陆面过程

塔克拉玛干沙漠腹地夏季夜间近地层存在逆温现象，日间气温变化情况与此相反；地表辐射平衡以正值为主，地表热量交换以湍流感热占主导地位，地表感热和潜热随着太阳高度角而变化，潜热最大值出现在凌晨，感热峰值出现在正午[45]. 塔克拉玛干沙漠地表感热通量和潜热通量的分布存在较大的季节性和区域性差异，春季感热通量在沙漠北部有减弱的、沙漠南部有增强的趋势，春季潜热通量在沙漠北部、西北部有减弱的趋势，沙漠南部、东南部有增强的趋势，而冬、夏、秋季变化趋势不是很大[46−47]. 在沙漠腹地人工绿地与自然沙面，地表热量输送主要以感热输送为主，但自然沙面感热通量更高、潜热通量更低[48].

2.2.2.1 沙漠太阳辐射

塔克拉玛干沙漠受人类活动的影响非常小，太阳辐射的影响因子主要与云和沙尘气溶胶有关[49]. 塔克拉玛干沙漠腹地总辐射、散射辐射和水平面直接辐射平均年总量分别为6 619 $MJ \cdot m^{-2}$、3 507.8 $MJ \cdot m^{-2}$和2 203.5 $MJ \cdot m^{-2}$，典型晴天总辐射日峰值分别为散射辐射的2.4倍和直接辐射的1.5倍，沙尘暴天散射辐射值增加到与总辐射基本一致[50]. 沙漠腹地的散射辐射表现为秋、冬季增加，并随太阳高度角的增大呈指数递增，大气质量的

增加而迅速降低[51]. 沙漠腹地紫外辐射平均年总量为320.7 MJ·m^{-2}，最大值为62.5 W·m^{-2}（6月），最小值为29.3 W·m^{-2}（12月）；户外紫外线（UVB）辐射年总量为8.59 MJ·m^{-2}，全年峰值（6月份）为2.51 W·m^{-2}. 春、夏季沙尘频发使紫外辐射日变化波动较大，在浮尘天、扬沙天和沙尘暴天，紫外辐射相对衰减26%、38%和45 %，沙尘导致的紫外辐射衰减是云量导致的紫外辐射衰减的2～4倍[52,53].

2.2.2.2 沙漠土壤热力作用

塔克拉玛干沙漠腹地平均土壤热容量、热传导率和热扩散率分别为1.559（±0.140）×10^6 J·m^{-3}·K^{-1}、0.234（±0.021）W·m^{-1}·K^{-1}和1.504（±0.110）×10^7 m^{-2}·s^{-1}；土壤热容量和热传导率具有明显的季节性变化，冬季值稳定且低而夏季值不稳定且高[54]. 塔克拉玛干沙漠地表发射率在靠近绿洲的地表最高，达到0.93，在绿洲与沙漠过渡带为0.91～0.92，沙漠其它地区为0.90～0.91，而沙漠腹地区域小于0.90[55]. 塔克拉玛干沙漠腹地和北缘地表反照年平均值为0.27[56]，反照率日均值的季节性变化明显，冬季高、夏季低. 沙漠腹地积雪覆盖期间地表反照率在0.18～0.97之间，日均值为0.60，其日变化更偏向反“J”型，呈现出上午大于傍晚的形态，平均早晚较差为0.13. 积雪地表反照率与地表温度表现出负相关关系，相关系数为-0.71，与5 cm深度土壤湿度呈负相关关系，相关系数为-0.74[57]. 塔克拉玛干沙漠北缘不同天条件下，气地表反照率也不同，雨天减小，雪天增大. 晴空指数≤0.3时，地表反照率波动很大，土壤湿度对沙漠北缘地表反照率日变化有影响，且地表反照率对0.097～0.13范围内的浅层土壤湿度响应敏感[56]. 沙漠北缘地表反照率（α）和比辐射率（ε）分别为0.27和0.91，这与塔克拉玛干沙漠腹地及北美大盆地沙漠一致，且α和ε值可从遥感产品获取[58].

塔克拉玛干沙漠腹地1 cm处土壤热通量年平均值为1.9 W·m^{-2}，年最大值为334.1 W·m^{-2}，年最小值为-184.2 W·m^{-2}，基本表现为夏季>春季>秋季>冬季；土壤热通量的各土层具有明显的日变化特征，并在不同天气情况下的日变化特征有一定的差异，在1 cm处受天气影响最显著[59]. 在日变化尺度上，沙漠腹地和北缘土壤热通量有明显日变化特征，1月沙漠腹地土壤热通量日平均变化幅度小于北缘，4月两地土壤热通量变化幅度较为接近，7、10月腹地土壤热通量变化幅度明显高于北缘[60].

2.2.2.3 沙漠二氧化碳和臭氧浓度

塔克拉玛干沙漠腹地地表白昼吸收CO_2、夜间排放CO_2，且吸收强度大于排放强度，CO_2通量受大气稳定性影响较大[61]. 沙漠腹地土壤呼吸速率整体偏低，但具有明显的昼夜波动性和季节变化特征[62]. 而沙漠北缘盐碱地和流沙地的土壤呼吸速率较低[63]. 土壤呼吸和微弱的气象条件相互作用，共同调节和控制近地层CO_2的浓度变化[64]. 冬季土壤呼吸日变化呈现出显著的单峰曲线，土壤呼吸速率与各层气温、0 cm地表温度之间均具有极其显著或显著的正线性关系，与5 cm土壤湿度之间具有较明显的线性关系，且0 cm地表温度对其贡献最大[65].

塔克拉玛干沙漠腹地地表臭氧的平均浓度在33.8 μg·m^{-3}～65.3 μg·m^{-3}之间，其平均值为49.0±0.45 .μg·m^{-3}；臭氧浓度变化具有周末效应现象，即夜间变化平缓，白天变化剧烈，09:00前后达到最低值，18:00前后达到最高值. 沙尘暴期间，臭氧浓度下降明显[18].

2.2.2.4 沙漠陆面过程关键参数

塔克拉玛干沙漠腹地动力学粗糙度的范围是2.7 ×10^{-5} m～8.0× 10^{-5} m，最佳值是3.88 ×10^{-5} m[54]. 塔克拉玛干沙漠北缘动力学粗糙度（z_{0m}）的最佳值为5.858×10^{-3} m，与Mojave沙漠、秘鲁沙漠、索诺兰沙漠、黑河地区、巴丹吉林沙漠相似. 塔克拉玛干沙漠北缘热力学粗糙度（z_{0h}）的峰值为1.965×10^{-4} m，与塔克拉玛干沙漠腹地不同. 年平均热传输附加阻尼（kB^{-1}）为2.5，与黑河地区地气相互作用实验研究（HEIFE）的戈壁及沙漠不同，但与青藏高原和国际水文和大气先行性试验（HAPEX）中的荒漠草原相似. z_{0m}和z_{0h}日变化不明显，但季节变化明显，热传输附加阻尼(kB^{-1})日变化和季节变化均不明显. z_{0m}受到局地风向影响明显. 在盛行风向和反盛行风向有许多起伏的沙丘，与z_{0m}峰值方向一致. 湍流动力输送系数（C_d）和湍流热力输送系数（C_h）日平均值（24小时）分别为6.34×10^{-3}和5.96×10^{-3}，高于塔克拉玛干沙漠腹地和戈壁区域，与HEIFE沙漠相似. 在盛行风向下（NNE–ESE），根据相似理论，平均C_d和C_h具有相同的量级. 在不同风向下，C_d和C_h与风速（U）、稳定度参数（z/L）的关系是不同的. 当风速低于3 m·s^{-1}时，且其最小值达到1 m·s^{-1}～2 m·s^{-1}时，C_d和C_h迅速降低. 应该指出，使用感热通量估算的ε值比使用其它方法估算要好[58].

2.2.2.5 沙漠湍流通量

沙漠腹地湍涡特征长度尺度在弱不稳定或近中性条件时最大，随不稳定程度的增强有明显减小的趋势，随

稳定程度的增加有先迅速减小后缓慢增加的趋势[66]. 近地层风速在沙尘暴过境期间具有先降低后增大的特点. 在10 m高度上，动量向下输送明显，热量输送只有很小的上升趋势；沙尘暴过境前，近地面为弱稳定的逆温层，空气处于暖干的状态，10 m高度上垂直气流表现为系统性的下沉运动，随着沙尘暴爆发，湍流交换显著增强，气流有上升运动趋势，但强度不大，仍以水平湍能为主[67].

在沙漠北缘大部分情况下湍流速度谱分布满足-2/3幂指数率，垂直方向高频段惯性副区符合程度更高，水平方向次之；CO_2和H_2O浓度则符合程度较低；温度谱与无因次频率总体上都具有很好的相关性. 垂直风速与径向风速的协谱斜率拟合值大多数情况下更接近-1，而在近中性层结条件下更符合-4/5斜线. 稳定层结条件下的协谱峰值比不稳定层结时更大，且约大一个量级；不稳定层结条件下高频段协谱近直线型下降. u谱对应的谱峰波长随稳定度增加而减小，v谱和T谱对应的谱峰波长随稳定度的增加没有规律性增减；u、v、w和T谱谱峰波长分别约67 m～827 m、69 m～2 417 m、4 m～54 m和12 m～661 m[68].

2.3　风沙物理研究

2.3.1　地表环境特征

塔克拉玛干沙漠地表土壤平均粒度为15.6 μm～250 μm，为细砂（125 μm～250 μm）、极细砂（62.5 μm～125 μm）、粗粉砂（31 μm～62.5 μm）、中粉砂（15.6 μm～31 μm）或者是其混合体[69]，其中，沙漠腹地和北缘贴地层（2 m高度以下）风沙流输沙以细砂（125 μm～250 μm）、极细砂（62.5 μm～125 μm）与粉砂为主，其中极细砂最多，占到输沙量的43.8%～75.5%. 各高度层中，粗砂（>250 μm）的含量极少[70]. 风沙流所搬运的沙粒的平均粒度都集中在62.5～125 μm的极细砂范围内，所有沙样的粒度都随着高度呈递减分布，近地面5 cm的平均粒度最大，2 m高度的平均粒度最小，说明在其它条件相同的情况下，粒度小的沙粒可以跳得更高[71].

塔克拉玛干沙漠腹地粒径大于0.3 mm的沙粒透明度较好，也有少量的沙粒透明度较差，如红色和黑色的沙粒，沙粒的表面磨蚀较为明显，棱角较少，圆度较好. 圆度值分布相对集中，大都在0.7～1.0之间，并且圆度值在0.8～0.9之间的沙粒比例最大，尤其以5 cm、10 cm和200 cm高度上的沙粒最为明显；粒径在0.125～0.3 mm之间的沙粒形状各种各样. 沙粒的圆度值集中分布在0.7～1.0之间，圆度值小于0.7的沙粒占到了41.49 %；粒径在0.074 mm～0.125 mm之间的沙粒中条形沙粒增多，沙粒的形状更加复杂，表面的磨蚀也越来越轻，棱角也更加尖锐[72].

2.3.2　风沙通量研究

塔克拉玛干沙漠腹地0 cm～100 cm风沙流结构完全符合指数分布，北缘则没有这样的特征. 风沙流输沙的粒径以细沙、极细沙、粉沙为主，其中极细沙占输沙量的43.8%～75.5 %. 输沙量随高度的增加呈下降趋势，沙漠腹地风沙运动主要集中在近地表20 cm～30 cm范围内，0 cm的输沙量可作为蠕移沙量，其约占总输沙量的11.6%，风沙流的蠕移输沙量方向分布与风向分布存在较大的差异. 风沙流中贴地层风速廓线受风沙相互作用的影响，不再符合对数分布，更加符合幂函数分布（$u=az^b$），拟合系数均大于0.93[70,71].

沙漠腹地起沙风向和输沙势主要分布在ENE、NE及E这3个方向上[73]. 沙尘天气（沙尘暴和扬沙）过程中，随着风速的增大，各高度层的输沙量也随之增大；两种天气过程中，沙粒的平均粒径在垂直高度上均呈现先减小后增大的趋势. 利用Hsensit风蚀传感器、风速仪、微梯度集沙仪器观测的资料分析发现，85 mm高度范围内，随风速的增加，跃移量/蠕移量之比呈负幂数函数下降，当风速在8.5 m·s^{-1}左右时，跃移量/蠕移量之比约为8～10；风速达到6.9 m·s^{-1}时，总跃移量最大值达1 952.01 g；风速达到7.6 m·s^{-1}时，总蠕移量最大值达211.79 g. 总跃移量和总蠕移量的比值随风速的增加呈指数递减，典型天气过程中不同风速下的总跃移量和总蠕移量比值约为8～24. 随风速的增大，输沙量越来越集中在0 mm～35 mm范围内. 集沙总量与Sensit风蚀传感器所记录的跃移颗粒数具有较好的线性关系，R^2值平均为0.605 3，全自动集沙仪在5 cm高度上的平均集沙效率为94.3%，观测期间，不同沙尘天气过程的沙尘输送量之间存在显著差异，过宽2 cm×高5 cm截面的沙尘最大水平通量约为190.335 kg，其最小值为1.2 kg. 沙尘天气中，输沙率的最大值出现在5 mm～15 mm高度，最小值出现在35 mm～85 mm高度. 扬沙天气中，风速大于9.2 m·s^{-1}时，输沙率最大值出现在0 mm～5 mm处. 沙尘暴天气中，拐点风速为7.5 m·s^{-1}，其小于7.5 m·s^{-1}时，输沙率的增加不显著，大于7.5 m·s^{-1}时，输沙率的增加显著[74−78]. 利用BSNE集沙仪观测到沙丘顶部和平沙地沙尘水平通量均随高度呈显著降低趋势，在这两种下垫面条件下，沙尘水平通量随高度的变化均较好地符合幂函数关系[79].

垂直沙通量随风速增加而增加，最大通量集中在午后. 当2 m风速为2 $m\cdot s^{-1}$时，沙漠腹地和北缘垂直沙尘通量接近3 $kg\cdot m^{-2}$；当2 m风速为6 $m\cdot s^{-1}$时，腹地和北缘垂直沙尘通量为10 $kg\cdot m^{-2}$，而水平沙尘通量的量级大于垂直沙尘通量. 当风速为2 $m\cdot s^{-1}$时，腹地和北缘水平沙尘通量为20 $kg\cdot m^{-2}$左右，其中腹地的值稍大；当风速为4 $m\cdot s^{-1}$时，腹地和北缘水平沙尘通量为40 $kg\cdot m^{-2}$左右，其中腹地的值较大；当风速为6 $m\cdot s^{-1}$时，腹地和北缘水平沙尘通量值分别为70 $kg\cdot m^{-2}$左右和65 $kg\cdot m^{-2}$左右[80].

沙漠腹地沙尘暴平均粒径在70 μm～85 μm的范围，由于沙丘和山谷的存在，近地层水平沙尘通量在较低高度内随着高度的增加而增加，但在32 m以上基本不变. 边界层垂直分布受风速控制，平均通量值在8 $kg\cdot m^{-2}$～14 $kg\cdot m^{-2}$范围内变化. 粉尘粒径PM_{100}及以下的占采集样品的60%～80 %，其中$PM_{0-2.5}$为0.9%～2.5%、PM_{0-10}为3.5%～7.0%、PM_{0-20}为5.0%～14.0%、PM_{0-50}为20%～40%. 沙尘垂直通量势平均为0.29 $kg\cdot m^{-2}$左右，从80 m向行星上层边界层和自由大气输送小于PM_{20}的颗粒[81].

2.3.3 近地层起沙输送机制

塔克拉玛干沙漠腹地平均风蚀气候因子指数（评价某一地区潜在风蚀能力的主要指标）值全年为28.3、夏季为13.9、冬季为0.7. 地表粗糙度平均值为6.32 10^{-5} m×10^{-5} m，由于地表粗糙度小，该地区的土壤风蚀程度加重了[82]. 塔克拉玛干沙漠腹地的临界摩擦速度为0.24 $m\cdot s^{-1}$，杨兴华等[83]发现Lettau输沙率公式的计算结果与实测值最接近. 春夏季地表起沙的临界摩擦速度为0.26 $m\cdot s^{-1}$，2 m高度的临界起沙风速约为4.1 $m\cdot s^{-1}$；沙尘通量的变化与风速及摩擦速度的变化具有一致性. 周成龙等[73]综合考虑了地表土壤粒径、土壤湿度、空气密度等因素，得出沙漠腹地2 m高度的临界摩擦速度值（0.24 $m\cdot s^{-1}$～0.36 $m\cdot s^{-1}$）和临界起沙风速值（3.9 $m\cdot s^{-1}$～5.9 $m\cdot s^{-1}$，均值为5.1 $m\cdot s^{-1}$）；沙漠腹地起沙阈值、最高值出现在夏季，次高值出现在冬季，最小高值出现在春季.

利用不同时间步长获取的临界起沙风速具有一定的差异，随着时间步长的缩小，临界起沙风速的获取越来越细化. 在不同的参数化方案中，临界起沙风速值不同，基于Marticorena和Shao方案得到的临界起沙风速均值分别为4.88 $m\cdot s^{-1}$和6.24 $m\cdot s^{-1}$[84−85]. 通过H11LIN型风蚀传感器获得的沙漠腹地最小起沙风速和临界起动摩擦速度分别为6.0 $m\cdot s^{-1}$和0.25 $m\cdot s^{-1}$[86].

塔克拉玛干沙漠跃移运动往往易发生在白天，跃移最活跃的时间为地方时11:30左右到16:30左右. 从2008年9月1日至2010年8月31日，跃移运动占全年总时间的3 %以上，并在春季和夏季的有大风运动月份趋于达到峰值. 然而，在冬季风速较弱的几个月里，跃移运动往往是最不活跃的. 在极端干旱的塔中地区，降水因素对减少沙粒跃移运动没有显著作用[87−88].

Stout开发的高斯时间分数等效法（间隔为1天），得到的摩擦速度阈值为3.03 $m\cdot s^{-1}$～5.62 $m\cdot s^{-1}$（野外试验观测方法），Kurosak方法得出的值为3.71 $m\cdot s^{-1}$～5.74 $m\cdot s^{-1}$（统计计算方法），Marticorena和Shao模型给出的值分别为4.87 $m\cdot s^{-1}$～4.90 $m\cdot s^{-1}$和5.82 $m\cdot s^{-1}$～6.78 $m\cdot s^{-1}$（模型参数化的方法）[85]. Stout、Kurosak、Marticorena和Shao方法的总水平沙尘通量估计值分别为1 311.9 $kg\cdot m^{-1}$、1 166.4 $kg\cdot m^{-1}$、1 279.9 $kg\cdot m^{-1}$和661.6 $kg\cdot m^{-1}$，而观测值为732.9 $kg\cdot m^{-1}$. 基于Stout、Kurosak、Marticorena和Shao方法的估计值和观测值的相关系数分别为0.75、0.79、0.77和0.83. Stout、Kurosak、Marticorena和Shao方法根据摩擦速度阈值估算的风沙跃移持续时间分别为8 211 min、6 575 min、7 567 min和3 463 min，而正确的时间分别为6 208 min、5 646 min、5 986 min和3 346 min.

风蚀的阈值（TWV）主要发生在白天（08:00～20:00），TWV以上风速频率表现出较大的季节变异性：春季（6.4%）>夏季（5.6%）>秋季（1.7%）>冬季（0.8%）. 累计起沙（DUP）在6月17日达50%，而9月1日增加至90%. 从2008年9月1日至2010年8月31日，均在4月1日至7月31日进行了观测，2年观测的结果均显示产生了75.4%的DUP. 研究表明，不同的风速时间分辨率会影响DUP的计算，当风速测量持续1分钟时，DUP为9.93×10^{6} $m^3\cdot s^{-3}$，持续5分钟时DUP为8.96×10^{6} $m^3\cdot s^{-3}$，持续10分钟时DUP为8.51×10^{6} $m^3\cdot s^{-3}$，持续15分钟时DUP为8.32×10^{6} $m^3\cdot s^{-3}$；DUP的季节变化规律呈：冬季>夏季>秋季>春季. 通过对昼夜DUP和不同观测时段风速的分析，发现主要偏差发生在清晨和晚上. 如果在10分钟或更长的时间间隔内测量平均风速，则评估风尘运动造成的损害会存在一定误差[89].

3 结 语

中国气象局在塔克拉玛干沙漠腹地建立了中国气象局乌鲁木齐沙漠气象研究所塔中大气环境观测试验站，

在塔克拉玛干沙漠及周边地区陆气相互作用、天气气候形成动力学机制、大气环境和沙漠区地表起沙及其输送机理等方面进行了长达十几年的研究，在沙漠气候与环境、沙漠陆气相互作用、风沙物理学等方面取得了较为系统的成果. 但还存在系统性不够完善、问题的揭示与理解不足、对野外实测的各类要素数据的分析不够深入、利用不充分等问题.

为了满足国家在区域发展、防灾减灾、气象服务、科学研究等方面日益增长的需求，需加强陆气相互作用研究和地表起沙输送过程观测试验，增强综合观测资料的应用能力，完善沙漠地区气候变化特征、风沙运移规律及沙漠微气象特点等方面的研究；同时需要获取改进区域数值预报模式所需的关键陆面过程参数以及结合遥感技术手段提高模式预报的能力；还需要利用现代空天地观测手段结合大数据处理方法，围绕沙漠地区沙尘气溶胶辐射强迫和沙漠大气之间的复杂耦合系统正、负反馈作用影响机理等科学问题进行深入研究.

参考文献：

[1] SUN J M, LIU T S. The age of the Taklimakan Desert[J]. Science, 2006, 312(5780): 1621.

[2] CHARNEY J G. Dynamics of deserts and drought in the Sahel[J]. Quarterly Journal of the Royal Meteorological Society, 1975, 101(428): 193-202.

[3] CHARNEY J G, QUIRK W J, CHOW S, et al. A comparative study of the effects of albedo change on drought in semi-arid regions[J]. Journal of the Atmospheric Sciences, 1977, 34(9): 1366-1385.

[4] HENDERSON-SELLERS A. Albedo changes—surface surveillance from satellites[J]. Climatic Change, 1980, 2(3): 275-281.

[5] CUNNINGTON W M, ROWNTREE P R. Simulations of the saharan atmosphere-dependence on moisture and albedo[J]. Quarterly Journal of the Royal Meteorological Society, 1986, 112(474): 971-999.

[6] HWANG S J. The effects of soil moisture on the energy balance at the bare soil surface[M]. Environmental Research Center, University of Tsukuba, 1995.

[7] WARNER T T. Desert meteorology[M]. Cambridge: Cambridge University Press, 2009.

[8] BAGNOLD R A. The physics of blown sand and desert dunes[M]. Berlin: Springer Netherlands, 1974.

[9] CHEPIL W S. Width of field strips to control wind erosion[J]. Kan Agric Exp Sta Tech bull, 1957: 92.

[10] T·ф·雅库波夫. 土壤风蚀及其防治[M]. 北京: 中国农业出版社, 1955: 5-26.
T·ф·Yakupov. Soil wind erosion and its prevention and control[M]. Beijing: China Agricultural Publishing House, 1955: 5-26. (in Chinese)

[11] 河村龙马. 飞砂の的研究. 东京大学理工学研究所报告[R]. 1951, 5(3/4): 95-112.
River village dragon horse. A study of flying sand の. Report of the Institute of Technology, University of Tokyo[R]. 1951, 5(3/4)95-112. (in Chinese)

[12] ZINGG A W. Wind tunnel studies of the movement of sedimentary material[R]. 5th Hydraulic Conference, Proceedings, Iowa Institute of Hydraulic, Iowa City, 1953: 111-135.

[13] OWEN R P. Saltation of uniform grains in air[J]. Fluid Mech, 1964, 20: 225-242.

[14] 贺大良, 高有广. 沙粒跃移运动的高速摄影研究[J]. 中国沙漠, 1988(1): 21-32.
HE D L, GAO Y G. The study of sand saltation movement with high velocity cinecamera[J]. Journal of Desert Research, 1988(1): 21-32. (in Chinese)

[15] 普宗朝, 张山清, 李景林, 等. 近47 a塔克拉玛干沙漠周边地区气候变化[J]. 中国沙漠, 2010, 30(2): 413-421.
PU Z C, ZHANG S Q, LI J L, et al. Climate change of area around Taklimakan Desert during 1961-2007[J]. Journal of Desert Research, 2010, 30(2): 413-421. (in Chinese)

[16] 周雪英, 贾健, 刘国强, 等. 1997-2017年塔克拉玛干沙漠腹地降水特征[J]. 中国沙漠, 2019, 39(1): 187-194.
ZHOU X Y, JIA J, LIU G Q, et al. Characteristics of precipitation at hinterland of Taklimakan Desert, China[J]. Journal of desert research, 2019, 39(1): 187-194. (in Chinese)

[17] 刘新春, 钟玉婷, 何清, 等. 塔克拉玛干沙漠腹地沙尘气溶胶质量浓度垂直分布特征[J]. 中国沙漠, 2012, 32(4): 1045-1052.
LIU X C, ZHONG Y T, HE Q, et al. Vertical distribution of dust aerosol mass concentration in hinterland of the Taklimakan Desert[J]. Journal of Desert Research, 2012, 32(4): 1045-1052. (in Chinese)

[18] 刘新春, 钟玉婷, 何清, 等. 塔克拉玛干沙漠腹地近地面臭氧浓度变化特征及影响因素分析[J]. 中国沙漠, 2013, 33(2): 626-633.
LIU X C, ZHONG Y T, HE Q, et al. The variation character, istics and influencing factors of surface ozone concentration in the Taklimakan Desert hinterland[J]. Journal of Desert Research, 2013, 33(2): 626-633. (in Chinese)

[19] 刘新春, 钟玉婷, 何清, 等. 塔克拉玛干沙漠腹地沙尘气溶胶质量浓度的观测研究[J]. 中国环境科学, 2011, 31(10): 1609-1617.
LIU X C, ZHONG Y T, HE Q, et al. Observation study on mass concentration of dust aerosols in the Taklimakan Desert Hinterland[J]. China Environmental Science, 2011, 31(10): 1609-1617. (in Chinese)

[20] 刘新春, 钟玉婷, 何清, 等. 塔克拉玛干沙漠腹地沙尘暴过程大气颗粒物浓度及影响因素分析[J]. 中国沙漠, 2011, 31(6): 1548-1553.
LIU X C, ZHONG Y T, HE Q, et al. Analysis on mass concentration of atmospheric particulate matter and its influencing factors in sandstorm process in the Taklimakan Desert hinterland[J]. Journal of Desert Research, 2011, 31(6): 1548-1553. (in Chinese)

[21] 刘新春, 代亚亚, 陈红娜, 等. 塔克拉玛干沙漠腹地沙尘天气过程粗细颗粒中水溶性离子组分垂直分布特征[J]. 生态环境学报, 2017, 26(6): 991-1000.
LIU X C, DAI Y Y, CHEN H N, et al. Analysis the vertical distribution characteristics on water soluble ions of coarse and fine component during, dust weather in the hinterland of the Taklimakan Desert[J]. Ecology and Environmental Sciences, 2017, 26(6): 991-1000. (in Chinese)

[22] 陆辉, 魏文寿, 刘明哲, 等. 塔克拉玛干沙漠腹地大气气溶胶中游离氧化铁的测定[J]. 地理科学, 2011, 31(8): 969-975.
LU H, WEI W S, LIU M Z, et al. Quantification and semi-quantification of iron-oxide minerals in aerosol particles in the hinterland of Taklimakan Desert[J]. Scientia Geographica Sinica, 2011, 31(8): 969-975. (in Chinese)

[23] 陆辉, 魏文寿, 刘明哲, 等. 塔克拉玛干沙漠腹地大气气溶胶散射特征研究[J]. 中国沙漠, 2010, 30(3): 660-667.
LU H, WEI W S, LIU M Z, et al. Aerosol scattering properties in the hinterland of Taklimakan Desert [J]. Journal of Desert Research, 2010, 30(3): 660-667. (in Chinese)

[24] 陆辉, 魏文寿, 崔彩霞, 等. 塔克拉玛干沙漠腹地黑碳气溶胶浓度[J]. 中国沙漠, 2014, 34(4): 1087-1093.
LU H, WEI W S, CUI C X, et al. Concentration of black carbon in the hinterland of the Taklimakan Desert[J]. Journal of Desert Research, 2014, 34(4): 1087-1093. (in Chinese)

[25] 霍文. 新疆沙尘暴天气演变特征及成因分析[D]. 乌鲁木齐: 新疆师范大学, 2011.
HUO W. The Analysis of the weather development characteristics and causes of sandstorm in Xinjiang[D]. Urumqi: Xinjiang Normal University, 2011. (in Chinese)

[26] 彭艳梅, 钟玉婷, 何清, 等. 大气气溶胶细粒子研究进展[J]. 沙漠与绿洲气象, 2013, 7(1): 69-74.
PENG Y M, ZHONG Y T, HE Q, et al. Research advance in fine particles of atmospheric aerosols[J]. Desert and Oasis Meteorology, 2013, 7(1): 69-74. (in Chinese)

[27] 彭艳梅, 王舒, 肖高翔, 等. 塔克拉玛干沙漠腹地塔中地区大气气溶胶散射系数影响因子[J]. 中国沙漠, 2018, 38(2): 384-392.
PENG Y M, WANG S, XIAO G X, et al. Impact factors of atmospheric aerosol scattering coefficient in the Tazhong area of the Taklimakan Desert[J]. Journal of Desert Research, 2018, 38(2): 384-392. (in Chinese)

[28] 彭艳梅, 高磊, 王舒, 等. 塔克拉玛干沙漠腹地气溶胶不同波段散射系数比较[J]. 沙漠与绿洲气象, 2018, 12(3): 26-32.
PENG Y M, GAO L, WANG S, et al. Comparison of aerosol scattering coefficients of different wave bands in the hinterland of the Taklimakan Desert[J]. Desert and Oasis Meteorology, 2018, 12(3): 26-32. (in Chinese)

[29] YANG X H, SHEN S H, YANG F, et al. Spatial and temporal variations of blowing dust events in the Taklimakan Desert[J]. Theoretical and Applied Climatology, 2016, 125(3): 669-677.

[30] LARE A R, NICHOLSON S E. A climatonomic description of the surface energy balance in the central sahel: Part I: shortwave radiation[J]. Journal of Applied Meteorology, 1990, 29: 123-137.

[31] WILLIAMS K J, BALLING J R C. Interaetion of desertification and climate[J]. Geneva: WMO and Nairobi: UNEP, 1994，230.

[32] 苏从先, 胡隐樵. 绿洲和湖泊的冷岛效应[J]. 科学通报, 1987, 10: 756-758.
SU C X, HU Y Q. Cold island effect in oases and lakes[J]. Scientific Bulletin, 1987, 10: 756-758. (in Chinese)

[33] 胡隐樵, 高由禧, 王介民, 等. 黑河实验(HEIFE)的一些研究成果[J]. 高原气象, 1994, 13(3): 225-236.
HU Y Q, GAO Y X, WANG J M, et al. Some achievements in scientific research during HEIFE[J]. Plateau Meteorological, 1994, 13(3): 225-236. (in Chinese)

[34] 张强. 极端干旱荒漠地区大气热力边界层厚度研究[J]. 中国沙漠, 2007, 27(4): 614-620.
ZHANG Q. Study on depth of atmospheric thermal boundary layer in extreme arid desert regions[J]. Journal of Desert Research, 2007, 27(4): 614-620. (in Chinese)

[35] 张强, 赵映东, 王胜, 等. 极端干旱荒漠区典型晴天大气热力边界层结构分析[J]. 地球科学进展, 2007, 22(11): 1150-1159.
ZHANG Q, ZHAO Y D, WANG S, et al. A study on atmospheric thermal boundary layer structure in extremely arid desert and

gobi region on the clear day in summer[J]. Advances in Earth Science, 2007, 22(11): 1150-1159. (in Chinese)

[36] 张强, 张杰, 乔娟, 等. 我国干旱区深厚大气边界层与陆面热力过程的关系研究[J]. 中国科学, 2011, 14(9): 1365-1374.
ZHANG Q, ZHANG J, QIAO J, et al. Relationship of atmospheric boundary layer depth with thermodynamic processes at the land surface in arid regions of China[J]. Science China: Earth Science, 2011, 14(9): 1365-1374. (in Chinese)

[37] 张强, 王胜. 西北干旱区夏季大气边界层结构及其陆面过程特征[J]. 气象学报, 2008, 66(4): 599-608.
ZHANG Q, WANG S. A study on atmospheric boundary layer structure on a clear day in the arid region in northwest China[J]. Acta Meteorologica Sinica, 2008, 66(4): 599-608.

[38] 李建刚, 奥银焕, 李照国, 等. 巴丹吉林沙漠夏季大气边界层结构[J]. 中国沙漠, 2014, 34(2): 488-497.
LI J G, AO Y H, LI Z G, et al. Characteristics of atmospheric boundary layer over the Badain Jaran Desert in summer[J]. Journal of Desert Research, 2014, 34(2): 488-497.

[39] 王敏仲, 魏文寿, 魏刚, 等. 风廓线雷达对塔克拉玛干沙漠沙尘及晴空湍流的探测研究[J]. 遥感技术与应用, 2014, 29(4): 581-586.
WANG M Z, WEI W S, WEI G, et al. Detection study of dust weather and clear-air turbulence in the hinterland of the Taklimakan Desert using a wind-profiling radar[J]. Remote Sensing Technology and Application, 2014, 29(4): 581-586. (in Chinese)

[40] WANG M Z, WEI W S, HE Q, et al. Summer atmospheric boundary layer structure in the hinterland of Taklimakan Desert[J]. Journal of Arid Land, 2016, 8(6): 846-860.

[41] WANG M Z, LU H, MING H, et al. Vertical structure of summer clear-sky atmospheric boundary layer over the hinterland and southern margin of Taklimakan Desert [J]. Royal Meteorological Society, 2016, 23: 438- 447.

[42] 张建涛, 何清, 王敏仲, 等. 塔克拉玛干沙漠腹地夜间稳定边界层观测个例分析[J]. 高原气象, 2018, 37(3): 826-836.
ZHANG J T, HE Q, WANG M Z, et al. A case analysis of nighttime stable boundary layer observation in the hinterland of Taklimakan Desert[J]. Plateau Meteorology, 2018, 37(3): 826-836. (in Chinese)

[43] 吴烨, 霍文, 何清, 等. 塔克拉玛干沙漠腹地自然沙面与人工绿地不同季节局地气候的差异性[J]. 水土保持通报, 2017, 37(2): 75-82+88.
WU Y, HUO W, HE Q, et al. Microclimate variability of natural sand and artificial green land in different seasons over Taklimakan Desert hinterland[J]. Bulletin of Soil and Water Conservation, 2017, 37(2): 75-82+88. (in Chinese)

[44] 金莉莉, 李振杰, 何清, 等. 塔克拉玛干沙漠腹地人工绿地中心区域与边缘地带小气候[J]. 中国沙漠, 2017, 37(5): 986-996.
JIN L L, LI Z J, HE Q, et al. Microclimate over the center and edge areas of the artificial shelter forest land in Taklimakan Desert[J]. Journal of Desert Research, 2017, 37(5): 986-996. (in Chinese)

[45] 魏文寿, 王敏仲, 何清, 等. 塔克拉玛干沙漠腹地近地边界层温湿廓线与热量平衡分析[J]. 科学通报, 2008(S2): 18-24.
WEI W S, WANG M Z, HE Q, et al. Analysis of temperature and humidity profile and heat balance of near-ground boundary layer in the hinterland of Taklimakan Desert[J]. Science Bulletin, 2008(S2): 18-24. (in Chinese)

[46] 王敏仲, 杨莲梅, 魏文寿, 等. 塔克拉玛干沙漠地表感热特征分析[J]. 干旱区资源与环境, 2009, 23(5): 172-178.
WANG M Z, YANG L M, WEI W S, et al. Analysis on characteristics of surface sensible heat flux in Taklimakan Desert[J]. Resources and Environment in Arid Areas, 2009, 23(5): 172-178. (in Chinese)

[47] 王敏仲, 魏文寿, 杨莲梅, 等. 塔克拉玛干沙漠地表潜热时空特征分析[J]. 中国沙漠, 2008, 28(5): 940-947.
WANG Z M, WEI W S, YANG L M, et al. Analysis on space-time characteristics of surface latent heat flux in Taklimakan Desert [J]. Journal of Desert Research, 2008, 28(5): 940-947. (in Chinese)

[48] 慕文玲, 霍文, 何清, 等. 塔中人工绿地与自然沙面感热通量和潜热通量差异性研究[J]. 干旱区资源与环境, 2017, 31(1): 115-120.
MU W L, HUO W, HE Q, et al. Research of sensible heat and latent heat fluxes in artificial vegetation and nature desert in Tazhong Area[J]. Journal of Arid Land Resources and Environment, 2017, 31(1): 115-120. (in Chinese)

[49] 李帅, 胡列群, 何清, 等. 塔克拉玛干沙漠腹地地表辐射收支特征研究[J]. 中国沙漠, 2012, 32(4): 1035-1044.
LI S, HU L Q, HE Q, et al. Surface radiation budget in hinterland of the Taklimakan Desert[J]. Journal of Desert Research, 2012, 32(4): 1035-1044. (in Chinese)

[50] 买买提艾力·买买提依明, 金莉莉, 李振杰, 等. 2007-2011年塔克拉玛干沙漠腹地太阳辐射观测研究[J]. 气候变化研究进展, 2014, 10(2): 87-94.
Ali Mamtimin, JIN L L, LI Z J, et al. Observational study of radiation on Taklimakan Desert hinterland from 2007 to 2011[J]. Climate Change Research, 2014, 10(2): 87-94. (in Chinese)

[51] 买买提艾力·买买提依明, 缪启龙, 金莉莉, 等. 塔克拉玛干沙漠腹地散射辐射特征[J]. 中国沙漠, 2013, 33(5): 1492-1500.

Ali Mamtimin, MIAO Q L, JIN L L, et al. Characteristics of diffuse reradiation at hinterland of the Taklimakan Desert[J]. Journal of Desert Research, 2013, 33(5): 1492-1500. (in Chinese)

[52] 何清, 金莉莉, 艾力. 买买提明, 等. 塔克拉玛干沙漠腹地太阳紫外UV-B辐射的观测与分析[J]. 中国沙漠, 2010, 30(3): 640-647.
HE Q, JIN L L, Ali Mamtimin, et al. Variation observation and analysis of solar UV-B radiation over the Taklimakan Desert hinterland[J]. Journal of Desert Research, 2010, 30(3): 640-647. (in Chinese)

[53] JIN L L, LI Z J, HE Q, et al. Characteristics of UV radiation at Tazhong of the Tarim Basin, west China[J]. Meteorology and Atmospheric Physics, 2014, 126: 91-103.

[54] LIU Y Q, HE Q, ZHANG H S, et al. Improving the Co LM in Taklimakan Desert hinterland with accurate key parameters and an appropriate parameterization scheme[J]. Adv Atmos Sci, 2012, 29(2): 381-390.

[55] 刘永强, 买买提艾力·买买提依明, 霍文, 等. 塔克拉玛干沙漠地表发射率及分布变化特征[J]. 沙漠与绿洲气象, 2014, 8(3): 1-7.
LIU Y Q, Ali Mamtimin, HUO W, et al. Variation characteristics of land surface emissivity on distribution and variation in Taklimakan Desert[J]. Desert and Oasis Meteorology, 2014, 8(3): 1-7. (in Chinese)

[56] 金莉莉, 李振杰, 买买提艾力·买买提依明, 等. 塔克拉玛干沙漠北缘地表反照率特征及参数化研究[J]. 资源科学, 2014, 36(5): 1051-1061.
JIN L L, LI Z J, Ali Mamtimin, et al. Variation characteristics and parameterization scheme of surface albedo over the northern margin of the Taklimakan Desert[J]. Resources Science, 2014, 36(5): 1051-1061. (in Chinese)

[57] 廖小荷, 何清, 金莉莉, 等. 塔克拉玛干沙漠腹地冬季积雪下垫面地表反照率及土壤温湿度变化特征[J]. 中国沙漠, 2018, 38(2): 393-400.
LIAO X H, HE Q, JIN L L, et al. Change of surface albedo, soil temperature and moisture under snow cover in the hinterland of Taklimakan desert in winter[J]. Journal of Desert Research, 2018, 38(2): 393-400. (in Chinese)

[58] JIN L L, LI Z J, HE Q, et al. Observed key surface parameters for characterizing land-atmospheric interactions in the northern marginal zone of the Taklimakan Desert, China[J]. Atmosphere, 2018, 9(12): 458.

[59] 张文斌, 买买提艾力·买买提依明, 何清, 等. 塔克拉玛干沙漠腹地土壤热通量变化特征[J]. 中国沙漠, 2016a, 36(6): 1666-1671.
ZHANG W B, Ali Mamtimin, HE Q, et al. Characteristics of soil heat flux in the hinterland of the Taklimakan Desert[J]. Journal of Desert Research, 2016, 36(6): 1666-1671. (in Chinese)

[60] 张文斌, 买买提艾力·买买提依明, 何清, 等. 塔克拉玛干沙漠不同区域土壤热通量比较[J]. 沙漠与绿洲气象, 2016, 10(2): 57-62.
ZHANG W B, Ali Mamtimin, HE Q, et al. Comparison of the soil heat flux variations in different areas over the Taklimakan Desert[J]. Desert and Oasis Meteorology, 2016, 10(2): 57-62. (in Chinese)

[61] 陈慧, 缪启龙, 买买提艾力·买买提依明, 等. 塔克拉玛干沙漠腹地春、夏季CO_2通量特征[J]. 干旱区地理, 2015, 38(3): 487-493.
CHEN H, MIAO Q L, Ali Mamtimin, et al. Variation CO_2 flux characteristics of Taklimakan Desert in spring and summer[J]. Arid Land Geography, 2015, 38(3): 487-493. (in Chinese)

[62] 郑新倩, 彭冬梅, 潘红林, 等. 塔克拉玛干沙漠腹地流沙下垫面土壤呼吸特征及影响因素分析[J]. 沙漠与绿洲气象, 2018, 12(5): 60-68.
ZHENG X Q, PENG D M, PAN H L, et al. Characteristics and effects factors of soil respiration with different time periods in the hinterland of the Taklimakan Desert[J]. Desert and Oasis Meteorology, 2018, 12(5): 60-68. (in Chinese)

[63] 杨帆, 买买提艾力·买买提依明, 杨兴华, 等. 新疆肖塘冬季土壤呼吸特征及影响因素[J]. 中国沙漠, 2015, 35(1): 195-202.
YANG F, Ali Mamtimin, YANG X H, et al. Characteristics and affecting factors of soil respiration in the northern margin of the Taklimakan Desert[J]. Journal of Desert Research, 2015, 35(1): 195-202. (in Chinese)

[64] 刘跃辉, 艾力·买买提依明, 杨帆, 等. 塔克拉玛干沙漠腹地冬季土壤呼吸及其驱动因子[J]. 生态学报, 2015, 35(20): 6711-6719.
LIU Y H, Ali Mamtimin, YANG F, et al. Environmental factors driving winter soil respiration in the hinterland of the Taklimakan Desert, China[J]. Acta Ecologica Sinica, 2015, 35(20): 6711-6719. (in Chinese)

[65] 刘跃辉, 买买提艾力·买买提依明, 何清, 等. 塔克拉玛干沙漠腹地冬季近地层CO_2浓度变化特征[J]. 中国环境科学, 2015, 35(5): 1328-1334.
LIU Y H, Ali Mamtimin, HE Q, et al. Variation characteristics of atmospheric CO_2 concentration of surface layer over the hinterland of Taklimakan Desert in winter[J]. China Environmental Science, 2015, 35(5): 1328-1334. (in Chinese)

[66] 温雅婷, 何宏让, 王春明, 等. 塔克拉玛干沙漠腹地湍流能量耗散率和结构函数参数特征[J]. 中国沙漠, 2014, 34(4): 1094-1101.
WEN Y T, HE H R, WANG C M, et al. Characteristics of turbulenceenergy dissipationrates and structure function parameters in the hinterland of the Taklimakan Desert[J]. Journal of Desert Research, 2014, 34(4): 1094-1101. (in Chinese)

[67] 温雅婷, 缪启龙, 何清, 等. 南疆一次强沙尘暴的近地层特征和湍流输送分析[J]. 中国沙漠, 2012, 32(1): 204-209.
WEN Y T, MIAO Q L, HE Q, et al. Surface layer characteristic sand turbulent flux transfer during a strong sand storm in south Xinjiang[J]. Journal of Desert Research, 2012, 32(1): 204-209. (in Chinese)

[68] 金莉莉, 李振杰, 何清, 等. 塔克拉玛干沙漠北缘夏季典型晴天近地层湍流能谱特征[J]. 中国沙漠, 2019, 39(6): 1-12.
JIN L L, LI Z J, HE Q, et al. Characteristic of surface-layer turbulence spectra on typical sunny days over the northern marginal zone of the Taklimakan Desert[J]. Journal of Desert Research, 2019, 39(6): 1-12. (in Chinese)

[69] 何清. 新疆大气气溶胶观测研究进展[A]. 中国气象学会大气成分委员会、中国气象科学研究院. 第26届中国气象学会年会大气成分与天气气候及环境变化分会场论文集[C]. 中国气象学会大气成分委员会、中国气象科学研究院: 中国气象学会, 2009: 22.
HE Q. Advances in aerosol observation in Xinjiang[A]. China Meteorological Society Atmospheric Composition Committee, China Institute of Meteorological Sciences. Proceedings of the 26th Annual Meeting of China Meteorological Society on Atmospheric Composition, Weather, Climate and Environmental Change[C]. China Meteorological Society Atmospheric Composition Committee, Chinese Academy of Meteorological Sciences: China Meteorological Society, 2009: 22. (in Chinese)

[70] 何清, 杨兴华, 艾力·买买提明, 等. 塔克拉玛干沙漠风蚀起沙观测研究——试验介绍与观测结果初报[J]. 中国沙漠, 2011, 31(2): 315-322.
HE Q, YANG X H, Ali Mamtimin, et al. Observation of dust emission by wind erosion in Taklimakan Desert[J]. Journal of Desert Research, 2011, 31(2): 315-322. (in Chinese)

[71] 杨兴华, 何清, 艾力·买买提明. 塔克拉玛干沙漠腹地塔中地区风沙流输沙特征研究[J]. 干旱区地理, 2011, 34(3): 479-485.
YANG X H, HE Q, Ali Mamtimin. Sand-transporting of sand flow at the Tazhong area in the hinterland of the Taklimakan Desert[J]. Arid Land Geography, 2011, 34(3): 479-485. (in Chinese)

[72] 赵聪敏. 塔克拉玛干沙漠沙粒形貌特征分析[D]. 乌鲁木齐: 新疆师范大学, 2012.
ZHAO C M. Research on morphology characteristic of sand particles in Taklimakan Desert[D]. Urumqi: Xinjiang Normal University, 2012. (in Chinese)

[73] 周成龙, 何清, 张爱强, 等. 塔克拉玛干沙漠腹地起沙阈值计算解析[J]. 沙漠与绿洲气象, 2014, 8(5): 53-57.
ZHOU C L, HE Q, ZHANG A Q, et al. The analytical calculation of the threshold for dust emission in the hinterland of the Taklimakan Desert[J]. Desert and Oasis Meteorology, 2014, 8(5): 53-57. (in Chinese)

[74] 康永德, 杨兴华, 何清, 等. 塔克拉玛干沙漠腹地贴地层风沙流结构研究[J]. 沙漠与绿洲气象, 2017, 11(2): 74-81.
KANG Y D, YANG X H, HE Q, et al. Research on wind-sand flow surface layer over the hinterland of the Taklimakan Desert[J]. Desert and Oasis Meteorology, 2017, 11(2): 74-81. (in Chinese)

[75] 康永德, 何清, 杨兴华, 等. 基于野外观测的风沙流跃移和蠕移运动规律研究[J]. 干旱区资源与环境, 2017, 31(5): 119-125.
KANG Y D, HE Q, YANG X H, et al. Research on saltation and creeping laws of wind-blown currents based on field observations[J]. Journal of Arid Land Resources and Environment, 2017, 31(5): 119-125. (in Chinese)

[76] 康永德, 杨兴华, 何清, 等. 塔中地区近地层风沙流的结构特征[J]. 水土保持通报, 2017, 37(3): 195-199.
KANG Y D, YANG X H, HE Q, et al. Structural characteristics of near surface wind blown sand in central Tarim Basin[J]. Bulletin of Soil and Water Conservation, 2017, 37(3): 195-199. (in Chinese)

[77] 康永德, 夏开伟, 杨兴华, 等. 近地层沙尘水平通量与集沙效率野外观测分析[J]. 农业工程学报, 2017, 33(13): 168-174.
KANG Y D, XIA K W, YANG X H, et al. Analysis of horizontal flux and sand collecting efficiency of sand dust near ground surface based on field observations[J]. Transactions of the Chinese Society of Agricultural Engineering (Transactions of the CSAE), 2017, 33(13): 168-174. (in Chinese)

[78] 康永德, 杨兴华, 何清, 等. 塔里木盆地塔中地区野外微梯度风沙流观测[J]. 干旱区研究, 2017, 34(3): 591-597.
KANG Y D, YANG X H, HE Q, et al. Micro-gradient field of wind-drift sand in Tazhong in the Tarim Basin[J]. Arid Zone Research, 2017, 34(3): 591-597. (in Chinese)

[79] 杨兴华, 何清, 李红军, 等. 塔里木盆地风蚀气候侵蚀力的计算与分析[J]. 中国沙漠, 2012, 32(4): 990-995.
YANG X H, HE Q, LI H J, et al. Calculation and analysis on wind erosion climatic erosivity in the Tarim Basin[J]. Journal of Desert Research, 2012, 32(4): 990-995. (in Chinese)

[80] 霍文. 塔里木盆地多种沙源类型沙通量异变特征研究[A]. 中国气象学会. 创新驱动发展提高气象灾害防御能力——S10大气物理学与大气环境[C]. 中国气象学会: 中国气象学会.
HUO W. Study on the variation characteristics of multi-type sand source dust flux in the Tarim Basin[A]. China Meteorological Society. Innovation-driven development to enhance meteorological disaster prevention capabilities ——S10 atmospheric physics

and atmospheric environment[C]. China Meteorological Society: China Meteorological Society2013: 760-768. (in Chinese)

[81] HUO W, HE Q, YANG F, et al. Observed particle sizes and fluxes of aeolian sediment in the near surface layer during sand-dust storms in the Taklamakan Desert[J]. Theoretical and Applied Climatology, 2017, 130(3-4): 735-746.

[82] 何清, 杨兴华, 艾力·买买提明, 等. 塔中地区土壤风蚀的影响因子分析[J]. 干旱区地理, 2010, 33(4): 502-508.
HE Q, YANG X H, Ali Mamtimin, et al. Impact factors of soil wind erosion in Tazhong Area[J]. Arid Land Geography, 2010, 33(4): 502-508. (in Chinese)

[83] 杨兴华, 何清, 艾力·买买提明. 塔克拉玛干沙漠塔中地区春夏季风蚀起沙研究[J]. 中国沙漠, 2010, 30(4): 770-776.
YANG X H, HE Q, Ali Mamtimin. Dust emission by wind erosion in spring and summer at Tazhong of Taklamakan Desert[J]. Journal of Desert Research, 2010, 30(4): 770-776. (in Chinese)

[84] 周成龙, 杨兴华, 钟昕洁, 等. 塔克拉玛干沙漠腹地沙尘天气特征[J]. 干旱区研究, 2017, 34(2): 324-329.
ZHOU C L, YANG X H, ZHONG X J, et al. Dust weather in hinterland of the Taklamakan Desert[J]. Arid Zone Research, 2017, 34(2): 324-329. (in Chinese)

[85] ZHOU C L, HE Q, HUO W, et al. Comparison of approaches for calculating the threshold velocity for sand movement based on field experiments in Xinjiang, China[J]. Arabian Journal of Geosciences, 2018, 11: 402.

[86] 杨兴华, 何清, 丁国锋, 等. 塔克拉玛干沙漠腹地风蚀起沙观测试验[J]. 沙漠与绿洲气象, 2012, 6(5): 67-72.
YANG X H, HE Q, DING G F, et al. The study on observation experiment of wind erosion over the hinterland of Taklimakan Desert[J]. Desert and Oasis Meteorology, 2012, 6(5): 67-72. (in Chinese)

[87] YANG X H, HE Q, Ali Mamtimin, et al. Diurnal variations of saltation activity at Tazhong: the hinterland of Taklimakan Desert[J]. Meteorology and Atmospheric Physics, 2013, 119(3): 177-185.

[88] YANG X H, Ali Mamtimin, HE Q, et al. Observation of saltation activity at Tazhong area in Taklimakan Desert, China[J]. Journal of Arid Land, 2013, 5(1): 32-41.

[89] ZHOU C L, Ali Mamtimin, YANG F, et al. Dust uplift potential in the Taklimakan Desert: an analysis based on different wind speed measurement intervals[J]. Theoretical and Applied Climatology, 2019, 137(1): 1449-1456.

责任编辑：艾合麦提·吾买尔